



Status of Turbulence Modeling for High-Speed Propulsion Flow Problems

N.J. Georgiadis
NASA Glenn Research Center
Cleveland, OH 44135 USA
Georgiadis@nasa.gov

W.A. Engblom, Embry-Riddle Aeronautical University

R.A. Baurle, NASA Langley

J.R. Edwards, N.C. State Univ.

A.Uzun, Florida State University

D.A. Yoder. M.A. Vyas, & J.R. DeBonis, NASA Glenn

The first author's work was Sponsored by the NASA Fundamental Aeronautics Program and the DoD Test Resource Management Center's (TRMC) Test and Evaluation /Science and Technology (T&E/S&T) Program through the High Speed Systems Test (HSST) area.

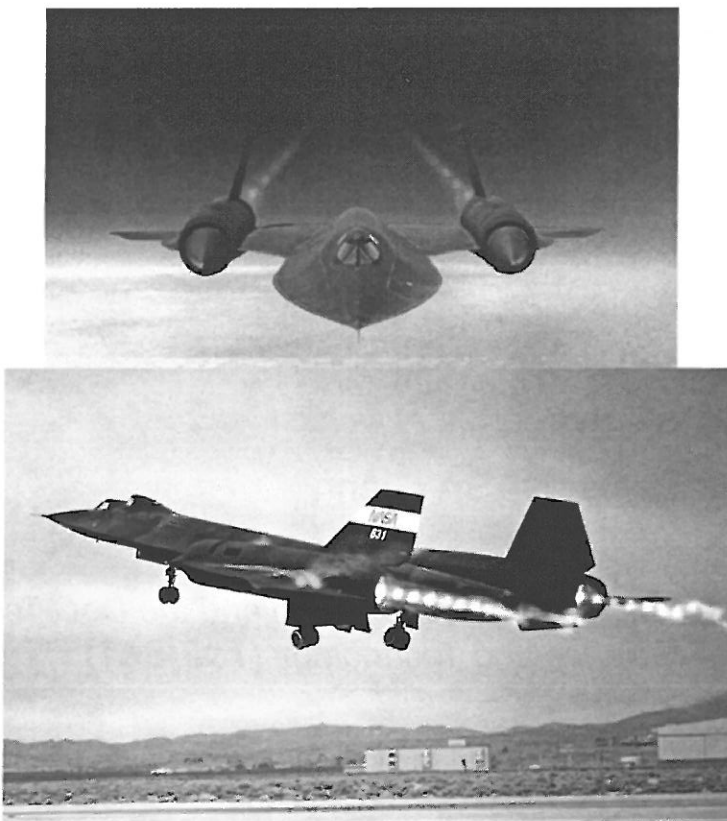


Introduction



- High speed aircraft are highly desirable for military and commercial applications.
- “Hypersonic” speed is frequently defined as Mach No. > 5

SR71 (Mach 3+):



X15 (Mach 6.7):



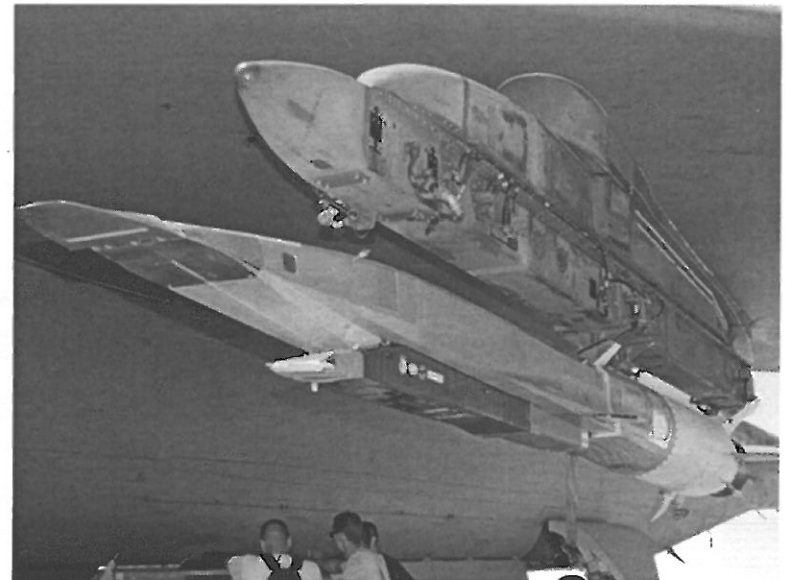
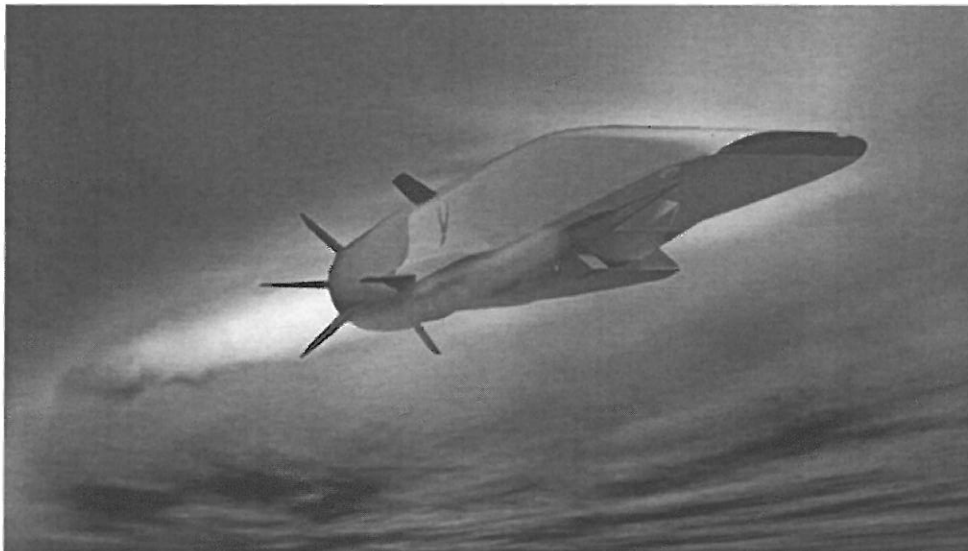


Introduction



- Hypersonic air-breathing propulsion is one of the most difficult R&D challenges facing the worldwide aeronautics community.

X51 Waverider:



- 1 out of 3 flights resulted in sustained combustion.
- Hydrocarbon fueled.

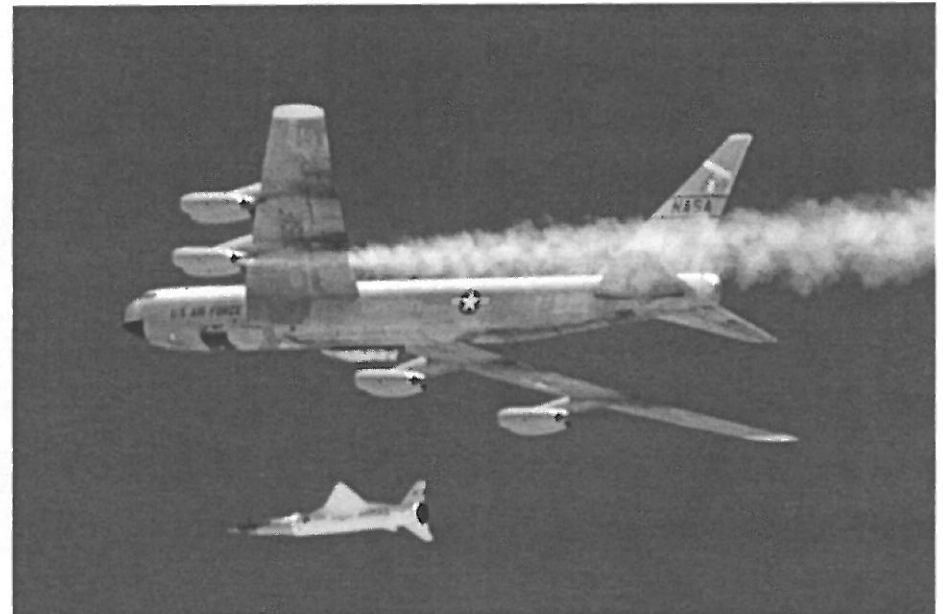
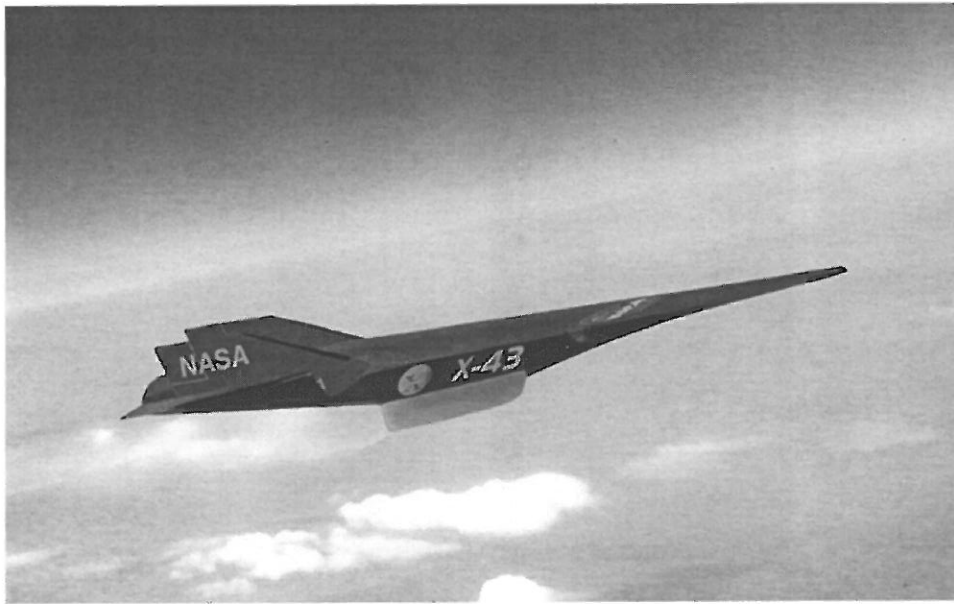


Introduction



- Current R&D uses ground tests and computational fluid dynamics (CFD) to prepare for flight tests.

X43:



- Flight 2 achieved Mach 7; Flight 3 achieved ~ Mach 10.
- Hydrogen fueled.



Introduction



- **High Speed / Hypersonic R&D uses flight tests, ground tests, and CFD ---- all have difficulties:**
 - 1. Flight tests: Expensive, difficult to instrument, very harsh environments for experimental aircraft that naturally lead to high failure rates.**
 - 2. Ground tests: Difficult to achieve actual flight conditions, facility interference effects, difficult to instrument.**
 - 3. CFD: Physical modeling is highly unproven – at best. Modeling of turbulence, chemistry, heat transfer, fluid-thermal-structural interactions is subject to high uncertainty.**



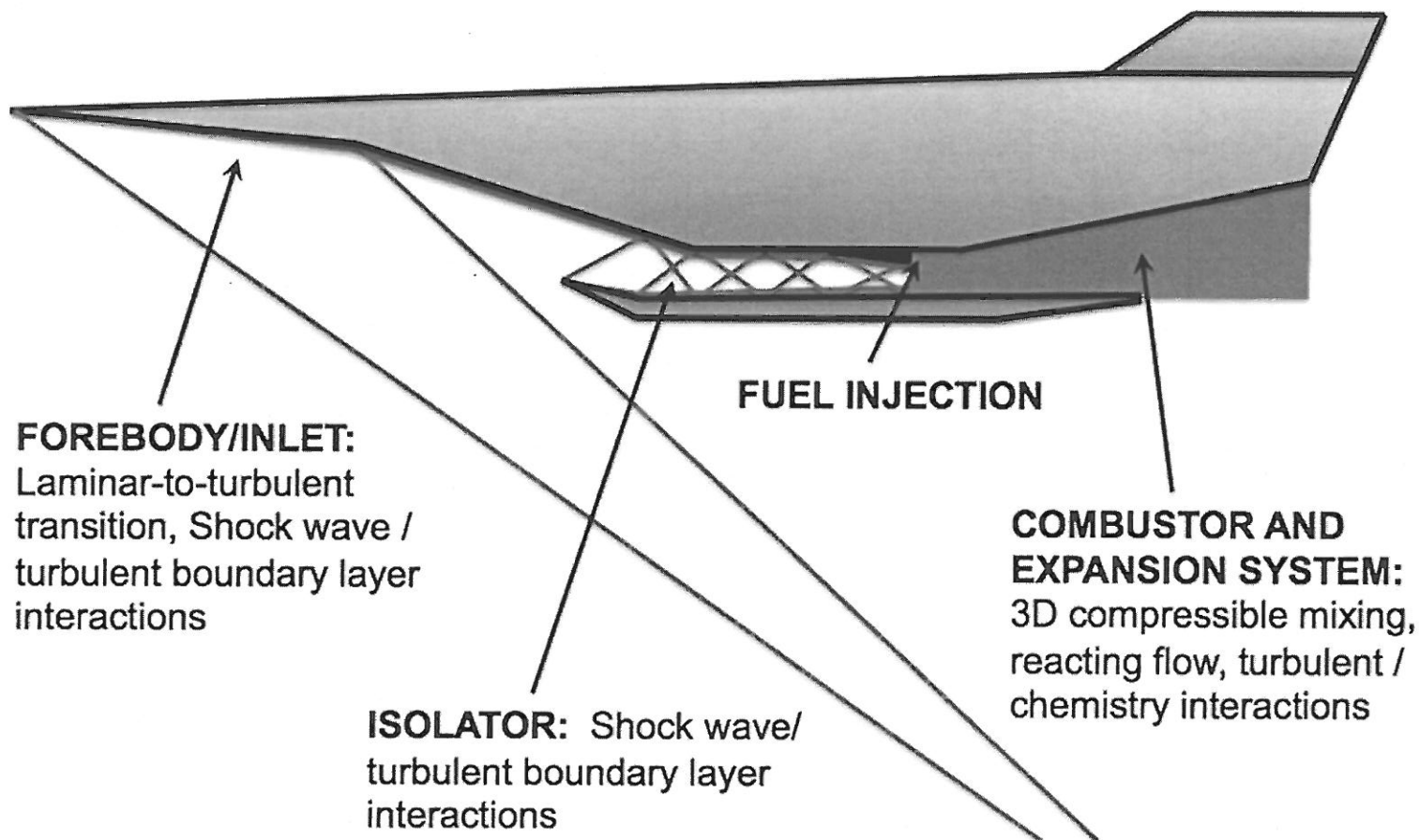
Introduction



- **Turbulence models remains one of the key pacing technologies in Computational Fluid Dynamics (CFD).**
- **An overview of key turbulence modeling areas for propulsion flows is presented.**
- **Emphasis is placed on “practical” state-of-the-art today:**
 - Standard practices using primarily RANS.
 - Promising new technology (i.e. LES, hybrid RANS/LES) that may be available for production use in near future.
 - Key shortfalls for which R&D is necessary.
- **Focus is placed on high-speed propulsion systems (i.e. scramjets); turbine engines are also addressed in less detail.**

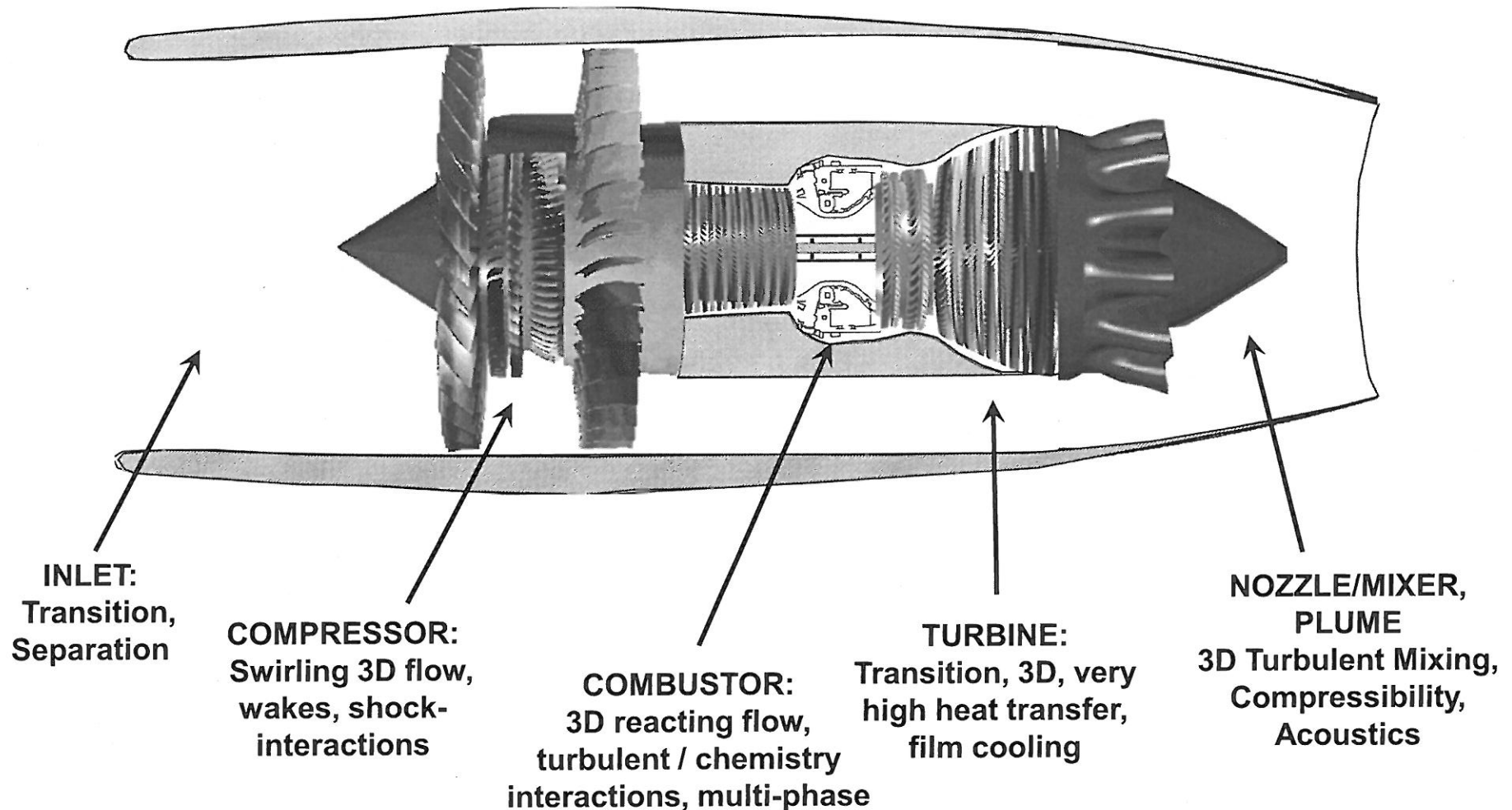


Key Turbulent Features of Scramjet Flowpaths





Key Turbulent Features of Turbine Engine Flowpaths





Presentation Outline



- **Overview of Turbulence Modeling in Use for Propulsion Flows**
 - RANS
 - LES and DNS
- **Boundary Layer Transition – Inlets and Turbines**
- **3D Boundary Layer Effects**
- **Shock-Wave /Turbulent Boundary Layer Interactions**
- **Combustor / Reacting Flows**
 - Scalar Transport
 - Turbulent / Chemistry Interactions
- **Exhaust System Modeling**
 - Jet and Mixing - RANS
 - LES-based Methods
- **Experimental Validation Data Needs**
- **Conclusions**



Navier-Stokes Equations

$$\frac{\partial \rho}{\partial t} + \frac{\partial}{\partial x_i}(\rho u_i) = 0$$

Continuity

$$\frac{\partial(\rho u_i)}{\partial t} + \frac{\partial}{\partial x_j}(\rho u_i u_j) = -\frac{\partial P}{\partial x_i} + \frac{\partial \tau_{ij}}{\partial x_j}$$

Momentum

$$\frac{\partial E_t}{\partial t} + \frac{\partial}{\partial x_j}(u_j(E_t + P)) = \frac{\partial}{\partial x_j}(u_i \tau_{ij}) - \frac{\partial q_j}{\partial x_j}$$

Energy

$$E_t = \rho e + \frac{1}{2} \rho u_i u_i$$



Navier-Stokes for Perfect Gas



$$P = \rho RT$$

Ideal Gas

$$\tau_{ij} = 2\mu S_{ij} - \frac{2}{3}\mu \frac{\partial u_j}{\partial x_j} \delta_{ij}$$

Newtonian Fluid

$$S_{ij} = \frac{1}{2} \left(\frac{\partial u_i}{\partial x_j} + \frac{\partial u_j}{\partial x_i} \right)$$

Rate of Strain

$$q_j = -k \frac{\partial T}{\partial x_j}$$

Fourier's Law



Reynolds Averaging

$$\bar{u}_i = \frac{1}{\tau} \int_t^{t+\tau} u_i dt$$

**Traditional
Reynolds-averaging**

$$\hat{u}_i = \frac{1}{\bar{\rho}\tau} \int_t^{t+\tau} \rho u_i dt$$

**Density weighting
(Favre averaging)**

$$\hat{f} = \frac{\overline{\rho f}}{\bar{\rho}}$$

(Favre averaging)



Modeled Turbulent Terms - RANS



$$-\overline{\rho u'_i u'_j} = \tau_{ij}^T$$

Reynolds Stress

$$-\overline{\rho u'_i h'} = q_i^T$$

Turbulent heat flux

These terms replace ALL turbulent effects in the momentum and energy equations.



Spatial Filtering

$$\bar{f}(x,t) = \int_D G(x - \xi, \Delta) f(\xi, t) d^3\xi$$

Filtering operation

$$\int_D G(x - \xi, \Delta) d^3\xi = 1$$

Filter function

$$\tilde{f} = \frac{\overline{\rho f}}{\bar{\rho}}$$

(Favre filtering)

Note that the Favre spatial filtering here and Favre Reynolds averaging look similar but refer to two very different operations.



Modeled Turbulent Terms - LES



$$-\bar{\rho}(\widetilde{u_i u_j} - \tilde{u}_i \tilde{u}_j) = \tau_{ij}^{sgs}$$

Subgrid Stress

$$\bar{\rho}(\widetilde{u_j h} - \tilde{u}_j \tilde{h}) = q_j^{sgs}$$

Subgrid heat flux

These terms replace only turbulent effects that are smaller than the numerical scheme and grid (hence called subgrid) can resolve.



Comparison of RANS and LES Equations

1 - Continuity



$$\frac{\partial \bar{\rho}}{\partial t} + \frac{\partial}{\partial x_i} (\bar{\rho} \hat{u}_i) = 0$$

RANS

$$\frac{\partial \bar{\rho}}{\partial t} + \frac{\partial}{\partial x_i} (\bar{\rho} \tilde{u}_i) = 0$$

LES



Comparison of RANS and LES Equations

2 - Momentum



$$\frac{\partial(\bar{\rho}\hat{u}_i)}{\partial t} + \frac{\partial}{\partial x_j}(\bar{\rho}\hat{u}_i\hat{u}_j) = -\frac{\partial\bar{P}}{\partial x_i} + \frac{\partial\bar{\tau}_{ij}}{\partial x_j} + \frac{\partial\tau_{ij}^T}{\partial x_j} \quad \text{RANS}$$

$$\frac{\partial(\bar{\rho}\tilde{u}_i)}{\partial t} + \frac{\partial}{\partial x_j}(\bar{\rho}\tilde{u}_i\tilde{u}_j) = -\frac{\partial\bar{P}}{\partial x_i} + \frac{\partial\bar{\tau}_{ij}}{\partial x_j} + \frac{\partial\tau_{ij}^{sgs}}{\partial x_j} \quad \text{LES}$$



Comparison of RANS and LES Equations

3 - Energy



$$\frac{\partial \hat{E}_t}{\partial t} + \frac{\partial}{\partial x_j} (\hat{u}_j (\hat{E}_t + \bar{P})) = \frac{\partial}{\partial x_j} (\hat{u}_i \bar{\tau}_{ij} + \hat{u}_i \bar{\tau}_{ij}^T) - \frac{\partial}{\partial x_j} (\bar{q}_j + q_j^T) \quad \text{RANS}$$

$$\frac{\partial \tilde{E}_t}{\partial t} + \frac{\partial}{\partial x_j} (\tilde{u}_j (\tilde{E}_t + \bar{P})) = \frac{\partial}{\partial x_j} (\tilde{u}_i \bar{\tau}_{ij} + \tilde{u}_i \tau_{ij}^{sgs}) - \frac{\partial}{\partial x_j} (\bar{q}_j + q_j^{sgs}) \quad \text{LES}$$



Major Differences Between Running RANS and LES



| RANS | LES |
|---|---|
| All turbulent stresses are replaced by the averaged effect (numerically diffusive) | Dominant turbulent stresses are calculated (numerically resolve unsteady behavior) – can't have too much diffusion or turbulence goes away. |
| Constant CFL – goal is to get to convergence as fast as possible. | Must run time accurately to capture time-varying turbulence. |
| Grids are packed to regions of high mean shear (stretching OK) | Best grids are uniform, isotropic – need to be of size to capture scales of interest. |
| Numerical scheme designed for reasonable accuracy, shock wave capturing, convergence characteristics. | Numerical scheme driven by need for high order of accuracy for resolving unsteady behavior. |



RANS Turbulence Modeling



- **Reynolds-Averaged Navier-Stokes (RANS) – replaces all unsteady turbulent motion with modeled turbulent stresses.**
- **Practical State of the art is two-equation models: $k-\varepsilon$, $k-\omega$, $k-\zeta$. Menter Shear-Stress Transport (SST) is popular “hybrid model” combining $k-\varepsilon$ and $k-\omega$.**
- **For subsonic/transonic external aerodynamics, one equation models such as Spalart-Allmaras are popular – not used as much in propulsion flows.**
- **Full Reynolds-Stress Models – offer more complete representation of 3-D turbulent stress field, but have not lived up to promise in terms of improved predictions.**
- **Explicit algebraic stress models (EASMs) solve 2-eqn models, but used additional relations to obtain “Reynolds-stress-like” behavior.**



Commonly Used RANS Models

1. Zero-equation (Algebraic): Cebeci-Smith, Baldwin-Lomax
 2. “Half-equation”: Johnson-King
 3. One-equation: Baldwin-Barth, Spalart-Allmaras
 4. Two-equation:
 - a) $k-\varepsilon$: Jones-Launder (standard), Chien, many others
 - b) $k-\omega$: Wilcox, Menter (BSL and SST)
 5. Explicit algebraic stress models (EASM)
 6. Reynolds-Stress closures
-
- The first 4 categories are “eddy viscosity models” where:

$$\tau_{ij}^T = -\overline{\rho u'_i u'_j} = \mu^T \left(2\hat{S}_{ij} - \frac{2}{3} \frac{\partial u_k}{\partial x_k} \delta_{ij} \right)$$



Spalart-Allmaras One Equation RANS Model



$$\frac{D\tilde{\nu}}{Dt} = c_{b1}\tilde{S}\tilde{\nu} + \frac{1}{\sigma}\frac{\partial}{\partial x_k}\left[(\nu + \tilde{\nu})\frac{\partial\tilde{\nu}}{\partial x_k}\right] + \frac{c_{b2}}{\sigma}\frac{\partial\tilde{\nu}}{\partial x_k}\frac{\partial\tilde{\nu}}{\partial x_k} - c_{w1}f_w\left(\frac{\tilde{\nu}}{d}\right)^2$$

$$\nu_T = \tilde{\nu}f_{v1}$$

$d =$ wall distance

$$f_{v1} = \frac{\chi^3}{\chi^3 + c_{v1}}$$

$$\chi = \frac{\tilde{\nu}}{\nu}$$

$$f_{v2} = 1 - \frac{\chi}{1 + \chi f_{v1}}$$

$$g = r + c_{w2}(r^6 - r)$$

$$\tilde{S} = S + \frac{\tilde{\nu}}{\kappa^2 d^2} f_{v2}$$

$$f_w = g \left[\frac{1 + c_{w3}^6}{g^6 c_{w3}^6} \right]^{1/6}$$

$$r = \frac{\tilde{\nu}}{\tilde{S}\kappa^2 d^2}$$

$$S = \sqrt{2\Omega_{ij}\Omega_{ij}}$$

$$c_{b1} = 0.1355, c_{b2} = 0.622, c_{v1} = 7.1, \sigma = 2/3,$$

$$c_{w1} = \frac{c_{b1}}{\kappa^2} + \frac{(1 + c_{b2})}{\sigma}, c_{w2} = 0.3, c_{w3} = 2, \kappa = 0.41$$



Jones-Launder Two-Equation k-ε RANS Model



$$\frac{D(\rho k)}{Dt} = \tau_{ij} \frac{\partial u_i}{\partial x_j} - \rho \varepsilon + \frac{\partial}{\partial x_j} \left[\left(\mu + \frac{\mu_t}{\sigma_k} \right) \frac{\partial k}{\partial x_j} \right] - 2\mu \left(\frac{\partial k^{1/2}}{\partial x_j} \right)^2$$
$$\frac{D(\rho \varepsilon)}{Dt} = C_{\varepsilon 1} \frac{\varepsilon}{k} \tau_{ij} \frac{\partial u_i}{\partial x_j} - C_{\varepsilon 2} \rho \frac{\varepsilon^2}{k} + \frac{\partial}{\partial x_j} \left[\left(\mu + \frac{\mu_t}{\sigma_\varepsilon} \right) \frac{\partial \varepsilon}{\partial x_j} \right] - 2 \frac{\mu \mu_T}{\rho} \left(\frac{\partial^2 u_j}{\partial x_k \partial x_k} \right)^2$$
$$\mu_t = C_\mu \rho \frac{k^2}{\varepsilon}$$

$$C_\mu = 0.09, \sigma_k = 1, \sigma_\varepsilon = 1.3, C_{\varepsilon 1} = 1.55, C_{\varepsilon 2} = 2.0$$

- Jones-Launder form is referred to as the “standard” k-ε model.
- Works well for attached boundary layers. Underestimates size of flow separation (early reattachments).
- Works reasonably well for mixing layers, jet flows. Compressibility corrections sometimes used for mixing problems at high convective Mach numbers.



Menter Two-Equation k- ω “Shear Stress Transport” (SST) RANS Model (1 of 2)



$$\frac{D(\rho k)}{Dt} = \tau_{ij} \frac{\partial u_i}{\partial x_j} - \beta^* \rho \omega k + \frac{\partial}{\partial x_j} \left[(\mu + \sigma_k \mu_t) \frac{\partial k}{\partial x_j} \right]$$

$$\frac{D(\rho \omega)}{Dt} = \frac{\alpha}{\nu_T} \tau_{ij} \frac{\partial u_i}{\partial x_j} - \beta \rho \omega^2 + \frac{\partial}{\partial x_j} \left[(\mu + \sigma_\omega \mu_t) \frac{\partial \omega}{\partial x_j} \right] + (1 - F_1) 2 \rho \sigma_{\omega 2} \frac{1}{\omega} \frac{\partial k}{\partial x_j} \frac{\partial \omega}{\partial x_j}$$

$$\mu_t = \min \left(\frac{\rho k}{\omega}, \frac{a_1 \rho k}{\Omega F_2} \right)$$

$$F_1^* = \tanh(\arg_1^4)$$

$$F_4 = \exp(-(R_y/120)^8)$$

$$F_1 = \max(F_1^*, F_4)$$

$$\arg_1 = \min \left[\max \left(\frac{k^{1/2}}{\beta^* \omega y}, \frac{500 \nu}{\omega y^2} \right), \frac{4 \rho \sigma_{\omega 2} k}{CD_{k\omega} y^2} \right]$$

$$CD_{k\omega} = \max(2 \rho \sigma_{\omega 2} \frac{\partial k}{\partial x_j} \frac{\partial \omega}{\partial x_j}; 1 \times 10^{-20})$$

$$F_2 = \tanh(\arg_2^2)$$

$$\arg_2 = \min \left(2 \frac{k^{1/2}}{\beta^* \omega y}, \frac{500 \nu}{\omega y^2} \right)$$



Menter Two-Equation $k-\omega$ “Shear Stress Transport” (SST) RANS Model (2 of 2)



- SST term comes from eddy viscosity expression. The hybrid $k-\omega$, $k-\varepsilon$ model without this term is referred to as the “Baseline” or BSL model.
- Inner model reduces to original Wilcox $k-\omega$ formulation. Outer model comes from transformed $k-\varepsilon$ model and is supposed to reduce to the “standard” $k-\varepsilon$ model but differs in cross diffusion term and diffusion coefficients.
- Model works quite well for attached boundary layers, mild separations, mixing flows (including jets). Numerically stable.
- All $k-\omega$ models may have an issue with artificial turbulence production behind strong normal shock.



Direct Calculation Methods



- **Direct Numerical Simulation (DNS)** – calculate all turbulent scales down to the Kolmogorov scale – impractical for engineering flows.
- **Large-Eddy Simulation (LES)** – directly calculate largest scales and reserve modeling for smallest “subgrid-scale” stresses – active research showing promise in combustor and jet plume regions.
- **Hybrid RANS/LES** – has become popular in recent years – most effective use has been for flows where RANS can be used in attached boundary layers and LES away from walls.
 - Demarcated or zonal hybrid RANS/LES – clear distinction is made between RANS and LES regions. Some physical mechanism is responsible for transition to turbulence. This was intent behind design of Detached Eddy Simulation (DES).
 - Continuous modeling – RANS and LES regions are not clearly separated – solution is expected to adjust, based on resolution. Desirable in theory, but difficult to achieve due to competing natures of RANS and LES.



Smagorinsky SGS Model



$$\tau_{ij}^{sgs} = 2(C_s \Delta)^2 \bar{\rho} \pi^{1/2} (\tilde{S}_{ij} - \frac{1}{3} \tilde{S}_{kk} \delta_{ij}) - \frac{2}{3} C_I \Delta^2 \bar{\rho} \pi \delta_{ij}$$

$$\mu^{sgs} = \bar{\rho} (C_s \Delta)^2 \rho \pi^{1/2}$$

$$\pi = \tilde{S}_{ij} \tilde{S}_{ij}$$

$$\Delta = (\Delta x \Delta y \Delta z)^{1/3}$$

$$\Delta = \max(\Delta x, \Delta y, \Delta z)$$

$$\Delta = \left[\frac{(\Delta x)^2 + (\Delta y)^2 + (\Delta z)^2}{3} \right]^{1/2}$$

- A few possibilities for the subgrid turbulent length scale:

- Note similarity of functional form to mixing-length RANS model (i.e. Cebeci-Smith); gradient-diffusion formulation; eddy viscosity that adds to laminar viscosity just as is done in RANS.
- The effect on N-S equations, however, is very different – only replacing subgrid turbulent stresses.



Transition Modeling

- Several RANS-based models tried over the past several years – some solving additional transport equations for intermittency, Re_θ .
- Some success for flows with high freestream turbulence intensity – i.e. turbine cascades where bypass transition is dominant mechanism.
- Modal growth situations not easily represented by RANS-based techniques.
- Work shown here is with a model based on the Menter SST k- ω turbulence model, with transition modifications by Langtry, Sjolander, & Menter.
- Our work with the baseline published model indicated difficulties: (1) inability to reproduce experimentally observed transition, (2) significant grid sensitivity, (3) inability to become fully turbulent beyond transition. New formulation described in Denissen, Yoder, Georgiadis, NASA TM 2008-215451.

TKE equation
$$\frac{\partial \rho k}{\partial t} + \frac{\partial \rho U_j k}{\partial x_j} = PTM \cdot \mathcal{P}_k - \beta^* \rho \omega k + \frac{\partial}{\partial x_j} \left((\mu + \sigma_k \mu_t) \frac{\partial k}{\partial x_j} \right)$$

$$PTM = 1 - 0.94(PTM1 + PTM2) F_3 \tanh((y^+/17)^2)$$

$$F_3 = e^{-\left(\frac{R_t}{5}\right)^2} (1 - P(R_t)) + \frac{1}{2} P(R_t)$$

**Modified model
formulation:**

$$P(R_t) = \frac{2.5}{\sqrt{2\pi}} e^{\frac{-(R_t-3)^2}{2}}$$

$$PTM1 = 1 - C_{PTM1} \begin{cases} [(3.28E - 4)Re_v - (3.94E - 7)Re_v^2 + (1.43E - 10)Re_v^3]; & Re_v < 1000 \\ [0.12 + (1E - 5)Re_v]; & Re_v > 1000 \end{cases}$$



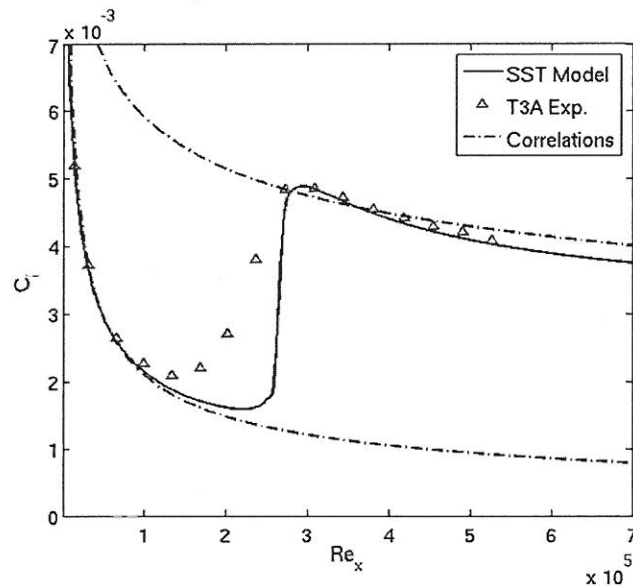
Boundary Layer Transition Model Incompressible Validation



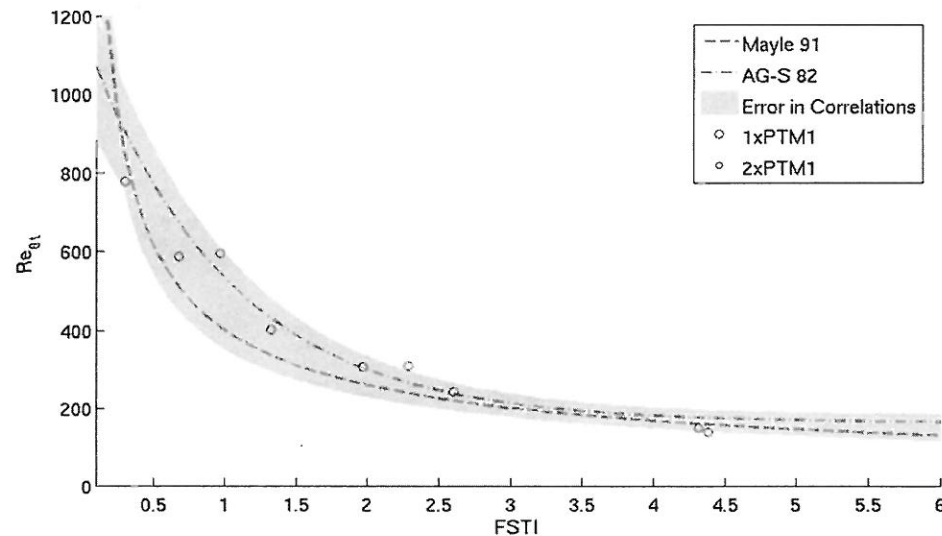
Incompressible Validation:

- Transition locations and skin friction examined for T3A benchmark data (ERCOFTAC)
- Several freestream intensities investigated.
- Grid sensitivity is high for incompressible cases.

C_f for FSTI = 2%



C_f Variation with FSTI



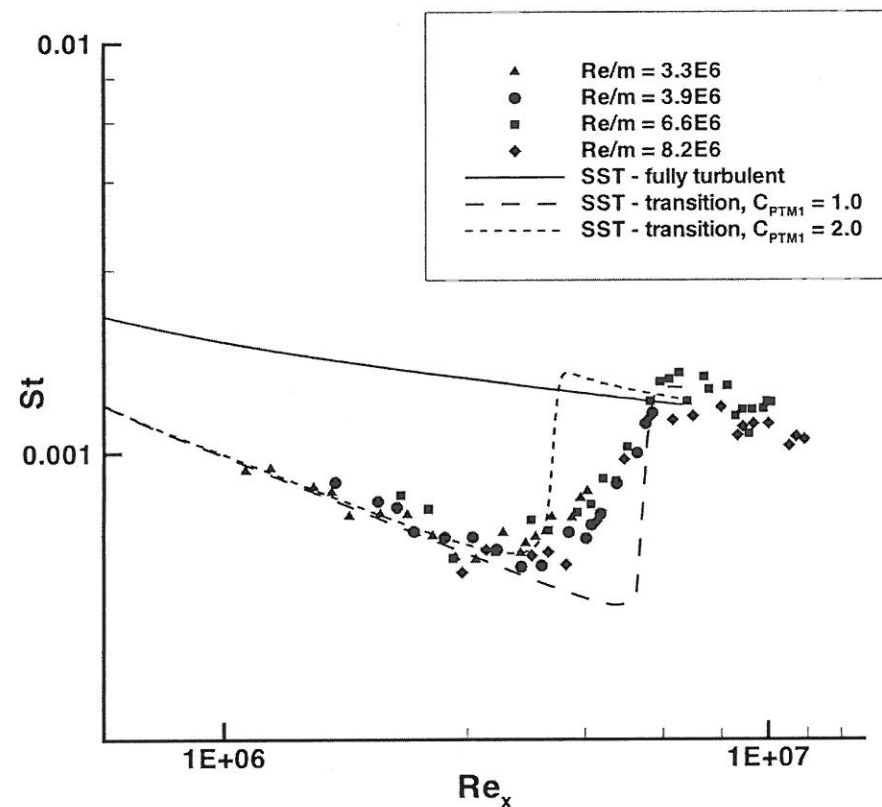


Boundary Layer Transition Model Hypersonic Validation



Hypersonic Validation:

- Mach 7.93, 7 degree straight cone investigated in AEDC Tunnel B, $T_w / T_o = 0.42$.
- Heat transfer measurements by Kimmel, JFE 1997.
- Integrated heat transfer: Transition-SST (6.7% error), Fully turbulent SST (18.5 % error).





Transition Modeling Conclusions



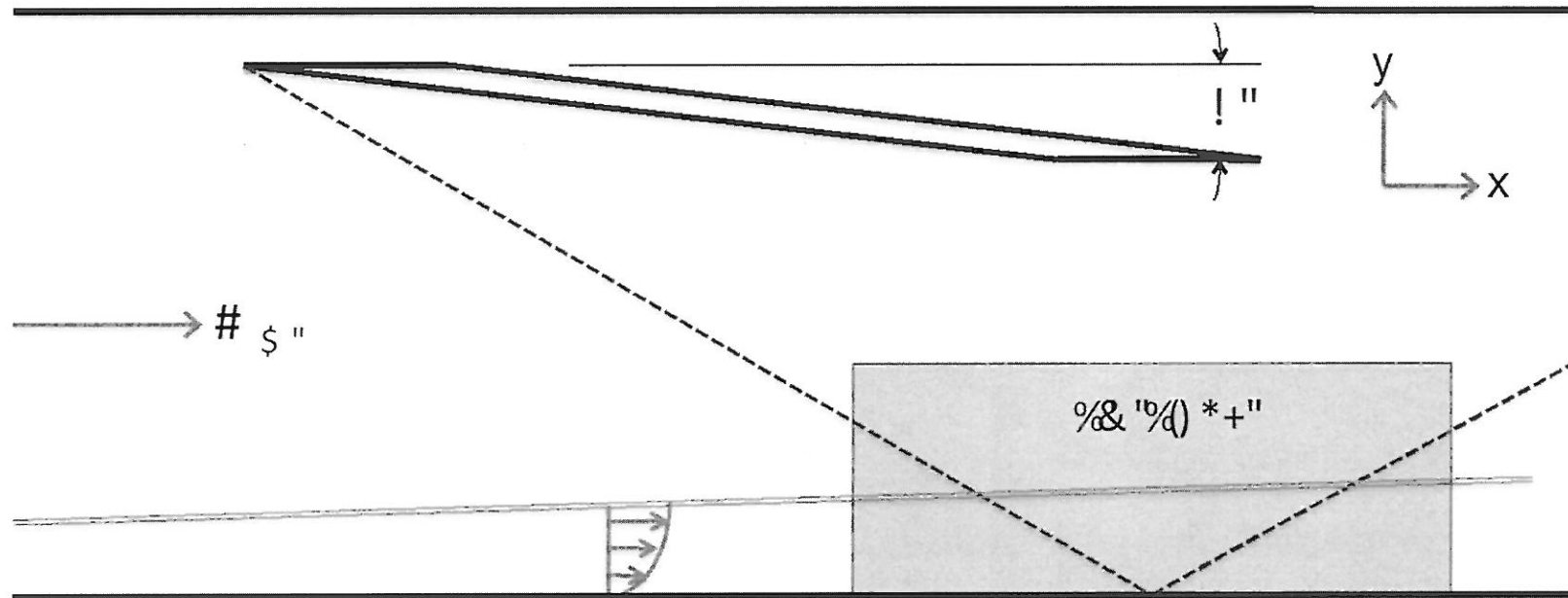
- **RANS-based models only applicable for bypass transition situations.**
- **Free-flight transition is normally modal growth – a reliable RANS-based method is not likely promising.**
- **LES is not promising either because accurately capturing the small disturbances is crucial – which LES will model/smear.**
- **Long Term Prospects – DNS, e^N methods.**



Shock-Wave Turbulent Boundary Layer Interactions (SWTBLIs)



- Pervasive to the entire hypersonic propulsion flowpath.
- Major challenge to RANS, LES and hybrid RANS-LES techniques.
- Nominally 2D problems are inherently 3D.

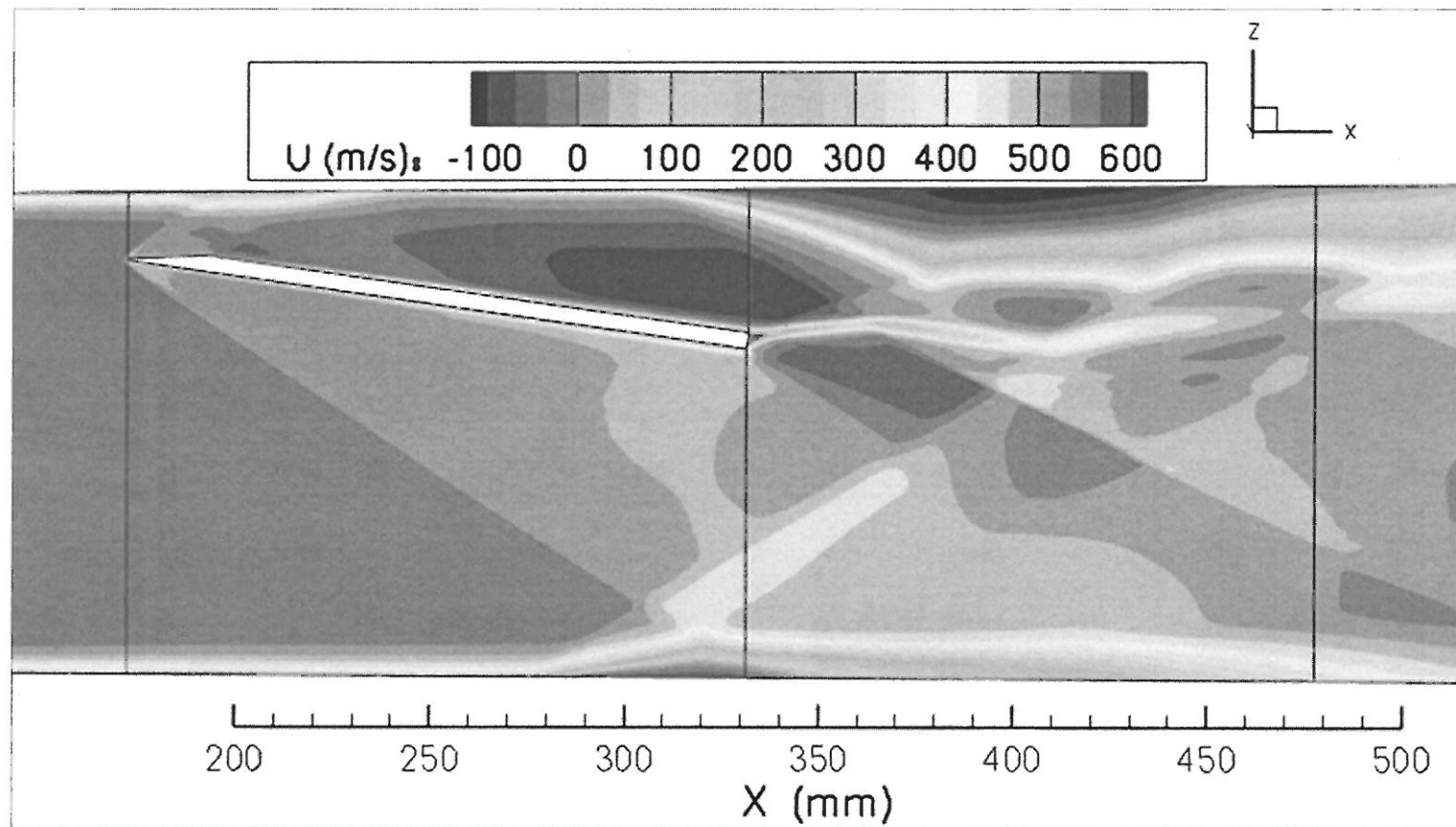




UFAST – Mach 2.25 Test Case



- 2010 AIAA Workshop: UFAST and U. of Michigan cases, targeted at representing supersonic aircraft inlets.
- Several organizations submitted results – RANS, LES, hybrids

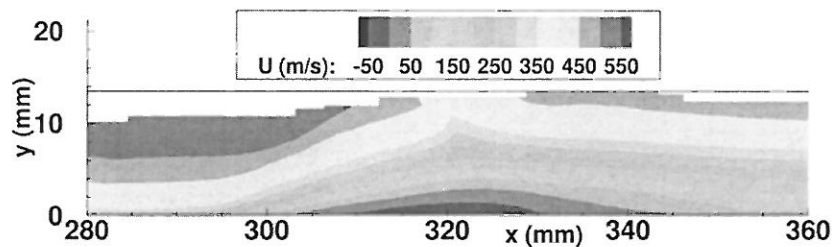




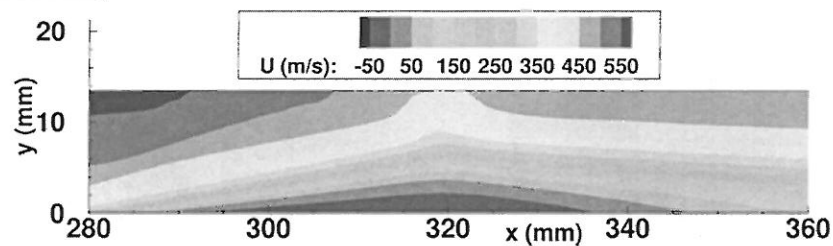
U Velocity Contours



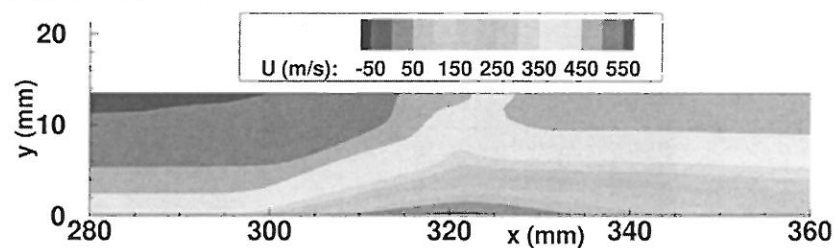
Experiment:



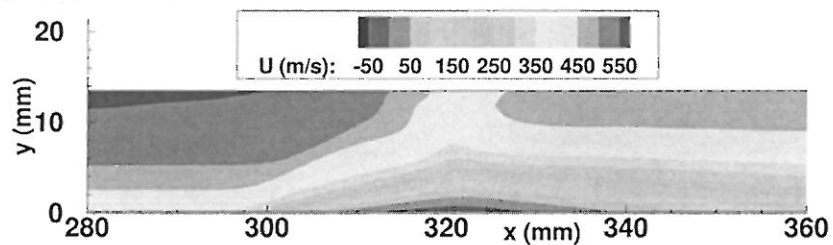
SST:



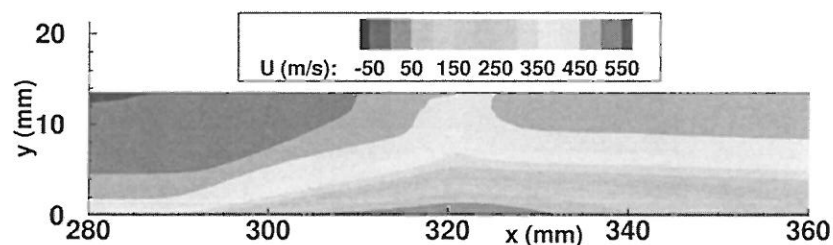
BSL:



SA:



k- ω ASM:



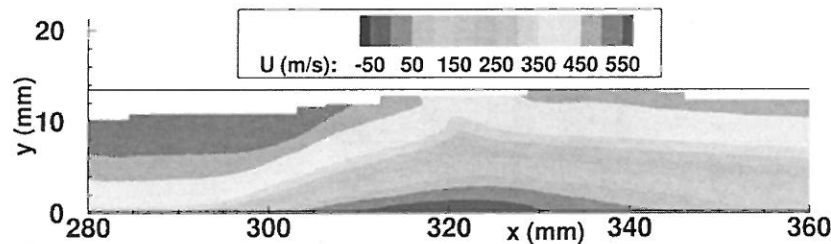


UFAST Velocity Contours

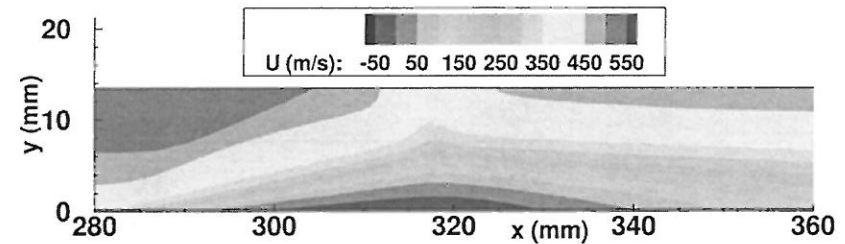


Exploring minor change to Menter SST model's stress limiter.

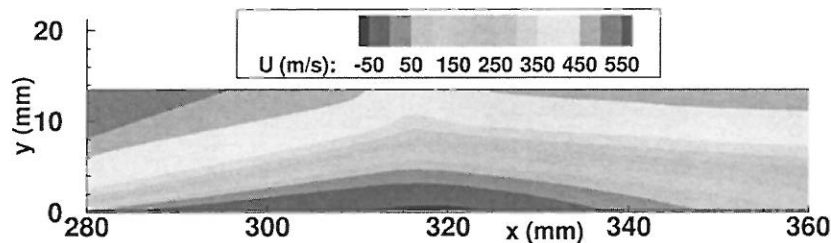
Experiment



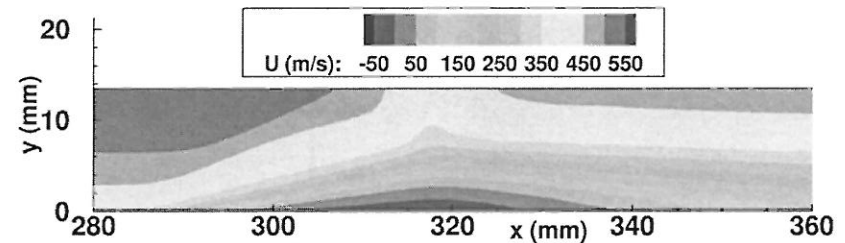
Menter SST $k-\omega$, $a_1 = 0.34$



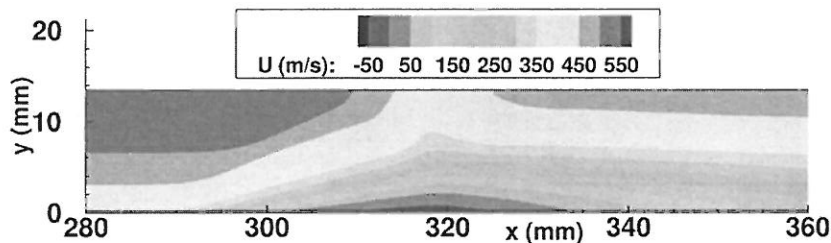
Menter SST $k-\omega$



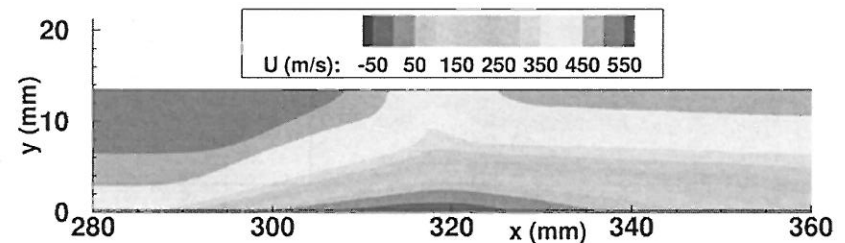
Menter SST $k-\omega$, $a_1 = 0.355$



Menter BSL $k-\omega$

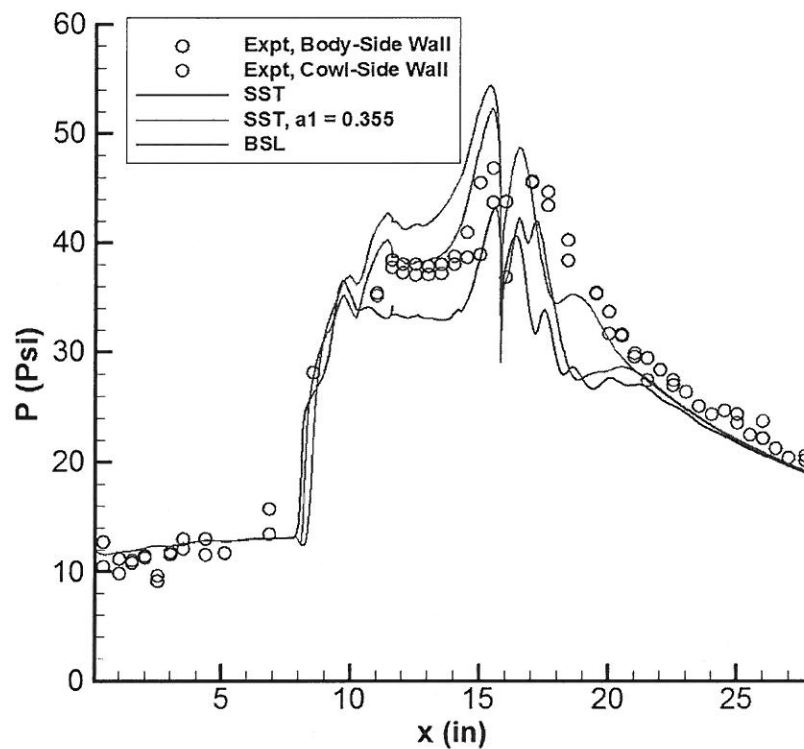
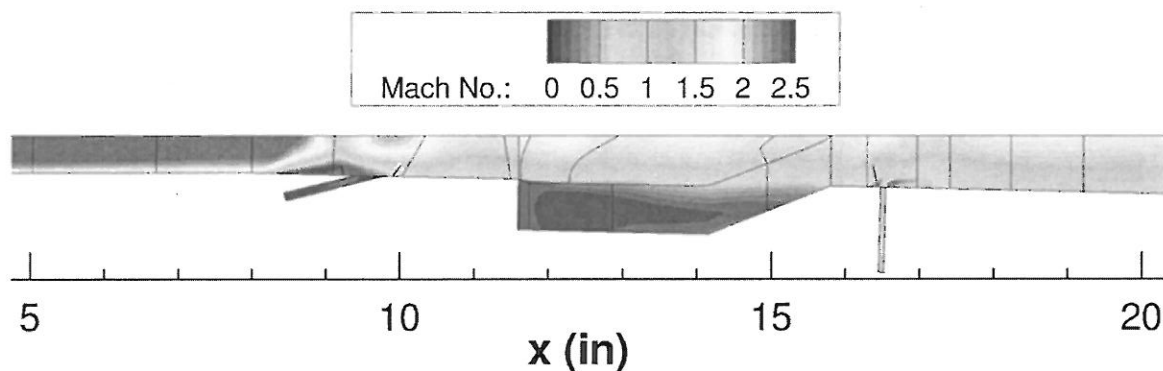


Menter SST $k-\omega$, $a_1 = 0.37$



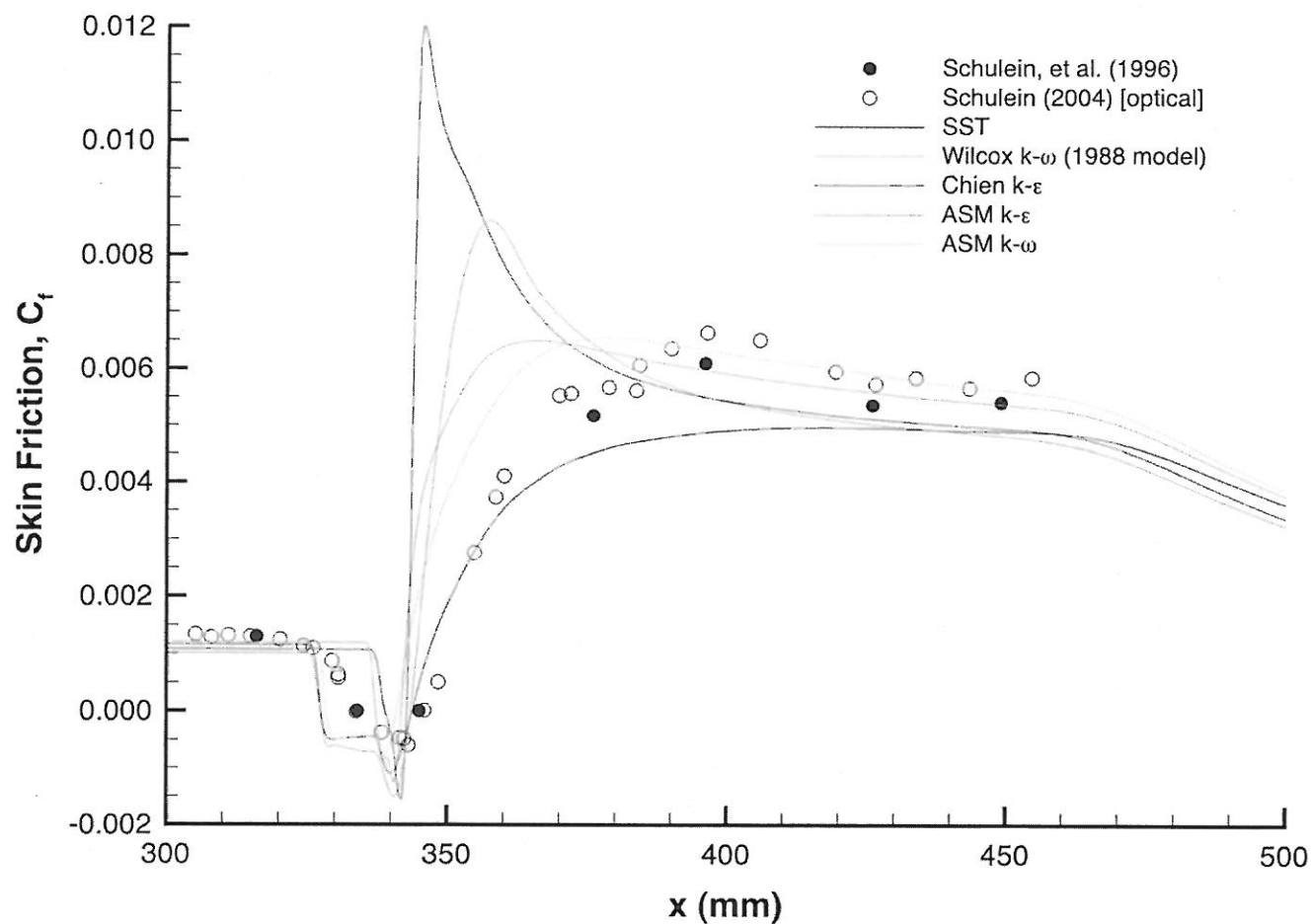


Hypersonic International Flight Research (HIFiRE) Direct-Connect Rig (HDCR) – Mach 5.8 Flight Case





Mach 5 SWTBLI





SWTBLI Modeling Conclusions



- k - ϵ models are generally overly optimistic on boundary layer health – smaller separations than expt.
- k - ω models usually work better for mild adverse pressure gradients, small separations, Menter SST predicts larger separations than expt.
- One equation models (i.e. SA) provide similar accuracy to multi-equation models.
- EASMs offer minimal improvement.
- Some success using LES at AIAA Workshop, inflow conditions & matching Re are significant challenges.
- Hybrid RANS-LES also being investigated – however, where is the switch from RANS to LES done?



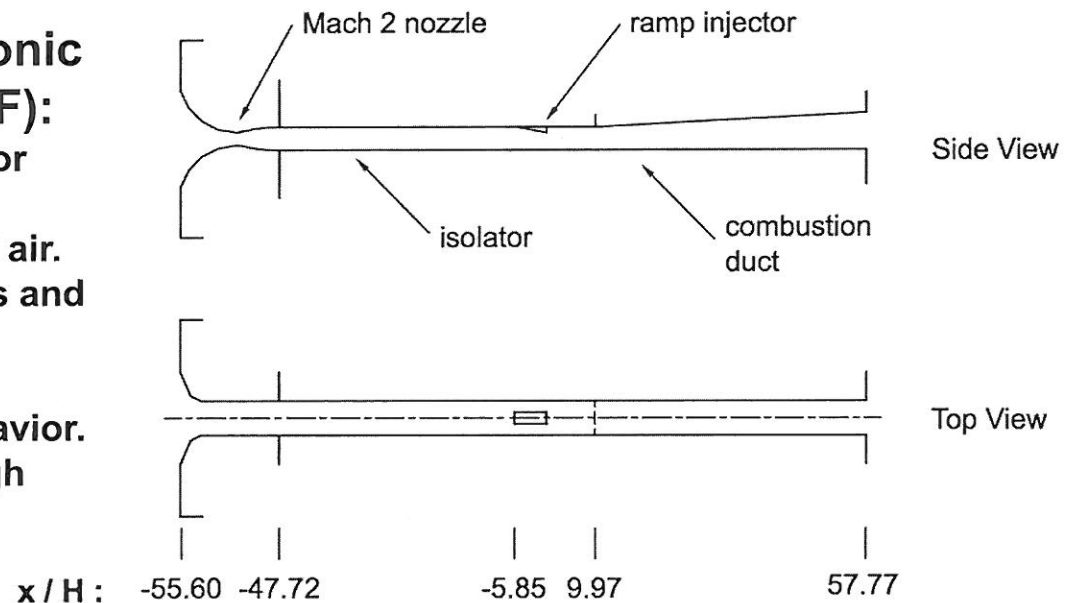
Combustor/Exhaust System Modeling



- Several interacting phenomena – kinetics, turbulence, heat transfer, thermal-structural effects.
- Practical state-of-the-art: Arrhenius form for reaction rates, 2 eqn turbulence model, constant Pr_t , Sc_t . Specified wall temperatures or heat fluxes.
- Most practical scramjet experiments: only centerline pressures available; More data and/or unit problems are desirable.

University of Virginia Supersonic Combustion Facility (UVA SCF):

- Mach 5 enthalpy, Mach 2 isolator
- overall pressure ratio ~ 4
- H_2 fueled, clean air and vitiated air.
- Documented heat transfer rates and wall temperatures.
- NASA-sponsored experiments focused on mode transition behavior.
- Continuing experiments through National Center.





Turbulent transport in energy and species equations



Turbulent heat flux: $q_i^T = -\overline{\rho u_i' h} = -k^T \frac{\partial \hat{T}}{\partial x_i}$

Turbulent Prandtl number: $Pr^T = \frac{\mu^T C_p}{k^T}$

Turbulent species flux: $m_i^T = -\overline{\rho u_i' w_1} = -D_{12}^T \frac{\partial \hat{w}}{\partial x_i}$

Turbulent Schmidt number: $Sc^T = \frac{\mu^T}{D^T}$

The turbulent Prandtl and Schmidt number are frequently set equal to 0.9. However, it is believed that realistic values can be significantly different for many flows – particularly in extreme environments such as scramjets.

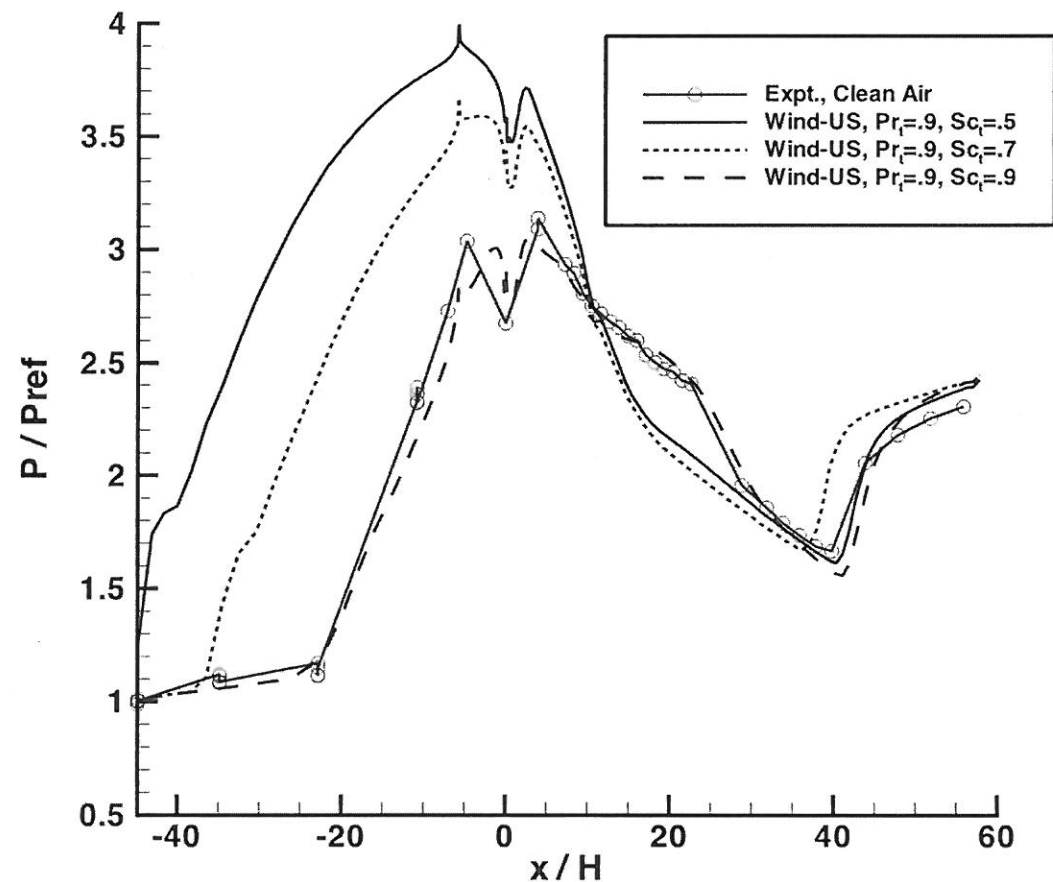


Sc_t Sensitivity for UVA SCF



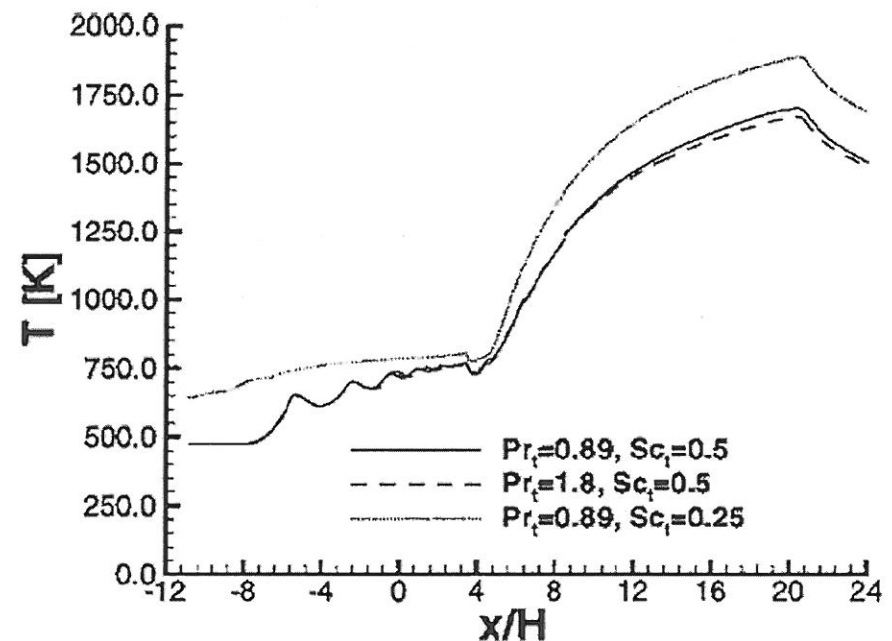
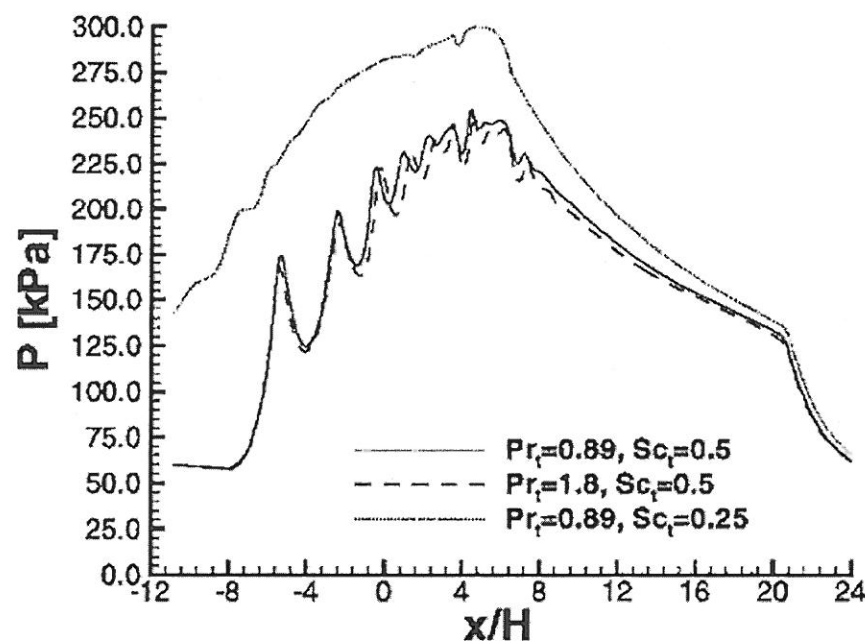
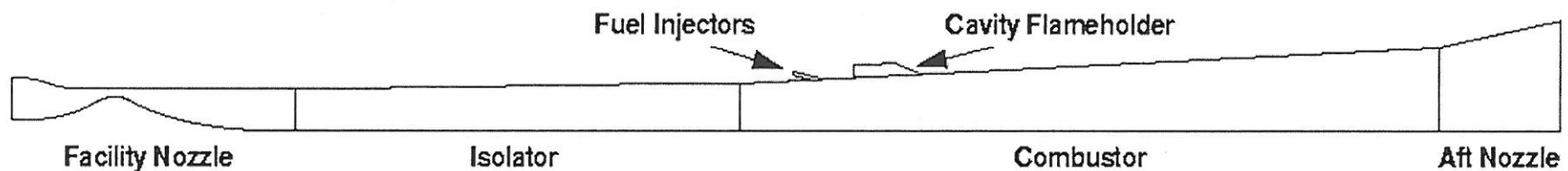
$\phi = 0.26$, Clean Air

| | |
|-------------|---------------------------|
| $x/H = -45$ | Beginning of isolator |
| $x/H = 0$ | Fuel exit/ ramp base |
| $x/H = 57$ | Nozzle exit to ambient |





Pr_t and Sc_t Sensitivity for USAF Scramjet



An “optimized” Pr_t and Sc_t for one case do not guarantee optimal performance for other ϕ 's, turb. models, kinetics, etc.

Figure: Courtesy of Robert A. Baurle, NASA LaRC



Pr_t Sensitivity for USAF Scramjet

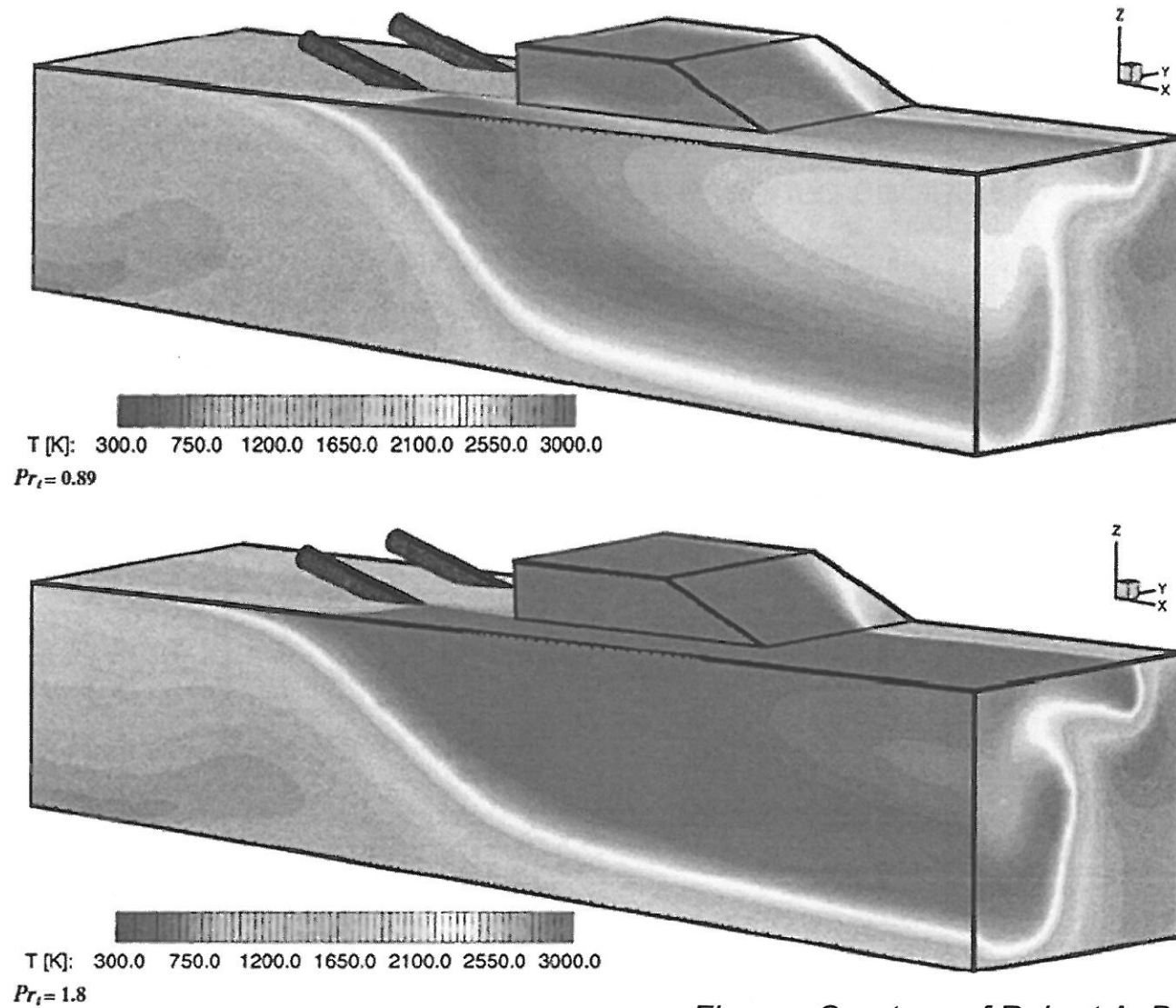


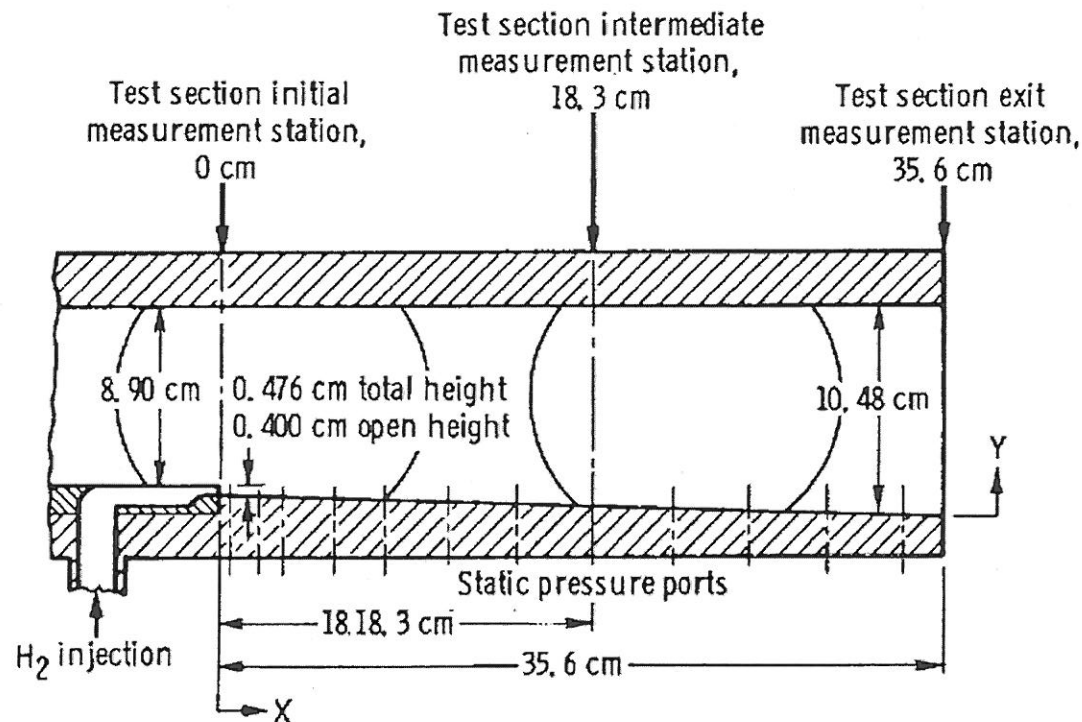
Figure: Courtesy of Robert A. Baurle, NASA LaRC



Burrows-Kurkov “Unit” Test Case



- Mach 2.4 vitiated air / sonic hydrogen experiment (1973).
- Used extensively for investigations/validation of H_2 -air CFD methods (kinetics, variable Pr_t , Sc_t , hybrid RANS-LES...), perhaps overused.
- Measurements of species concentrations and temperatures.



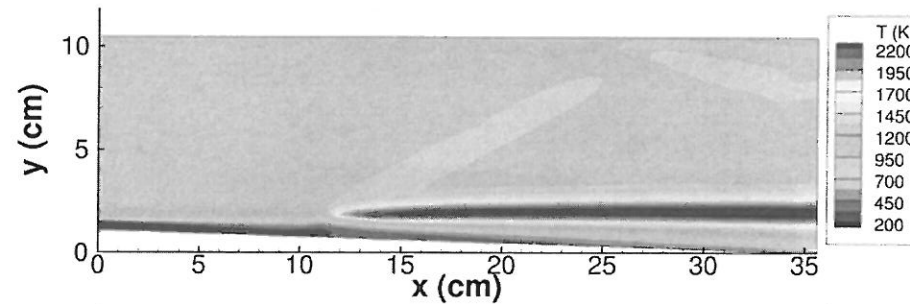


Sc_t Effects on Ignition Point for Burrow-Kurkov Test Case

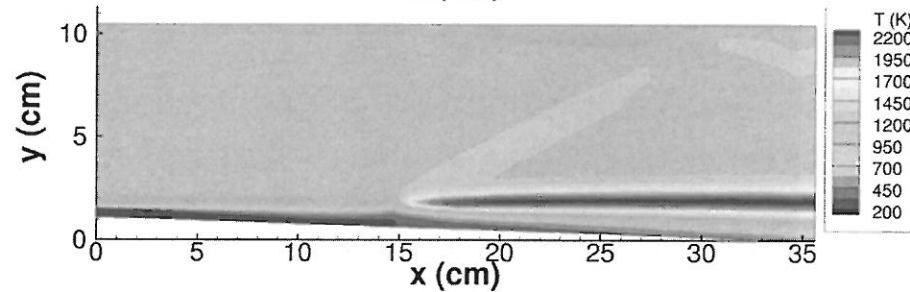


$Pr_t = 0.7$ (constant) for all cases

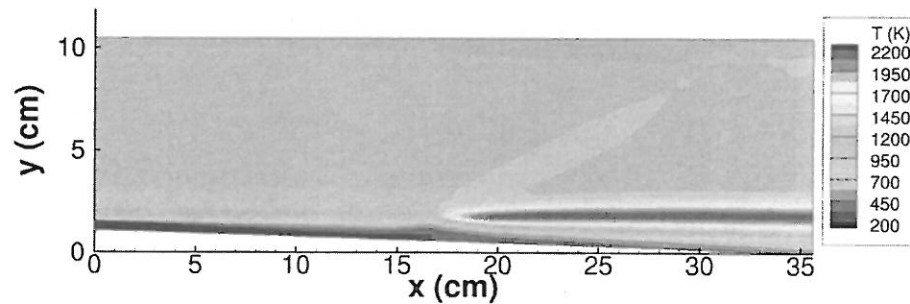
$Sc_t = 0.5$



$Sc_t = 0.7$



$Sc_t = 0.9$

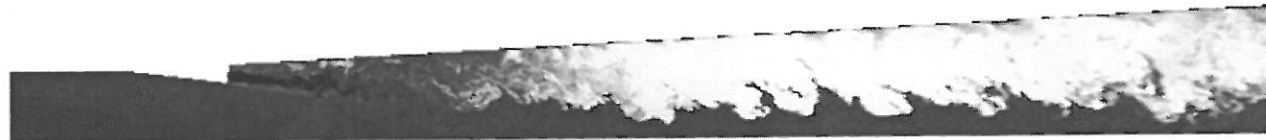




Hybrid RANS/LES Calculations of UVA Dual-Mode Scramjet, $\Phi = 0.17$



Temperature



Eddy
viscosity

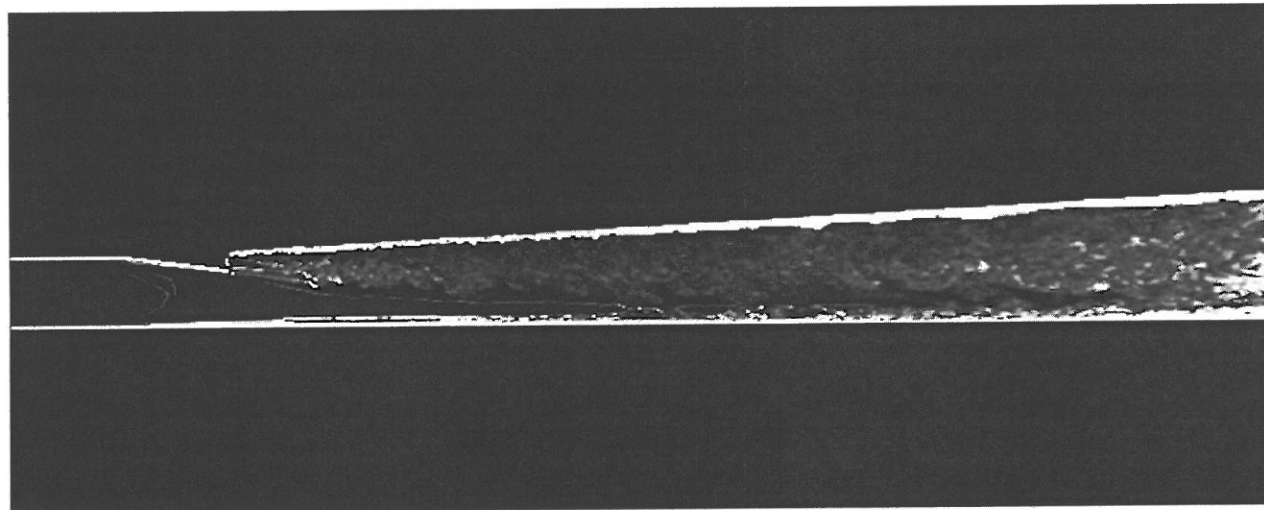


Figure: Courtesy of Jack Edwards, NCSU



Hybrid RANS/LES Calculations of UVA Dual-Mode Scramjet, $\Phi = 0.17$



CARS comparisons (temperature): ($X/H = 6, 12, 18$)

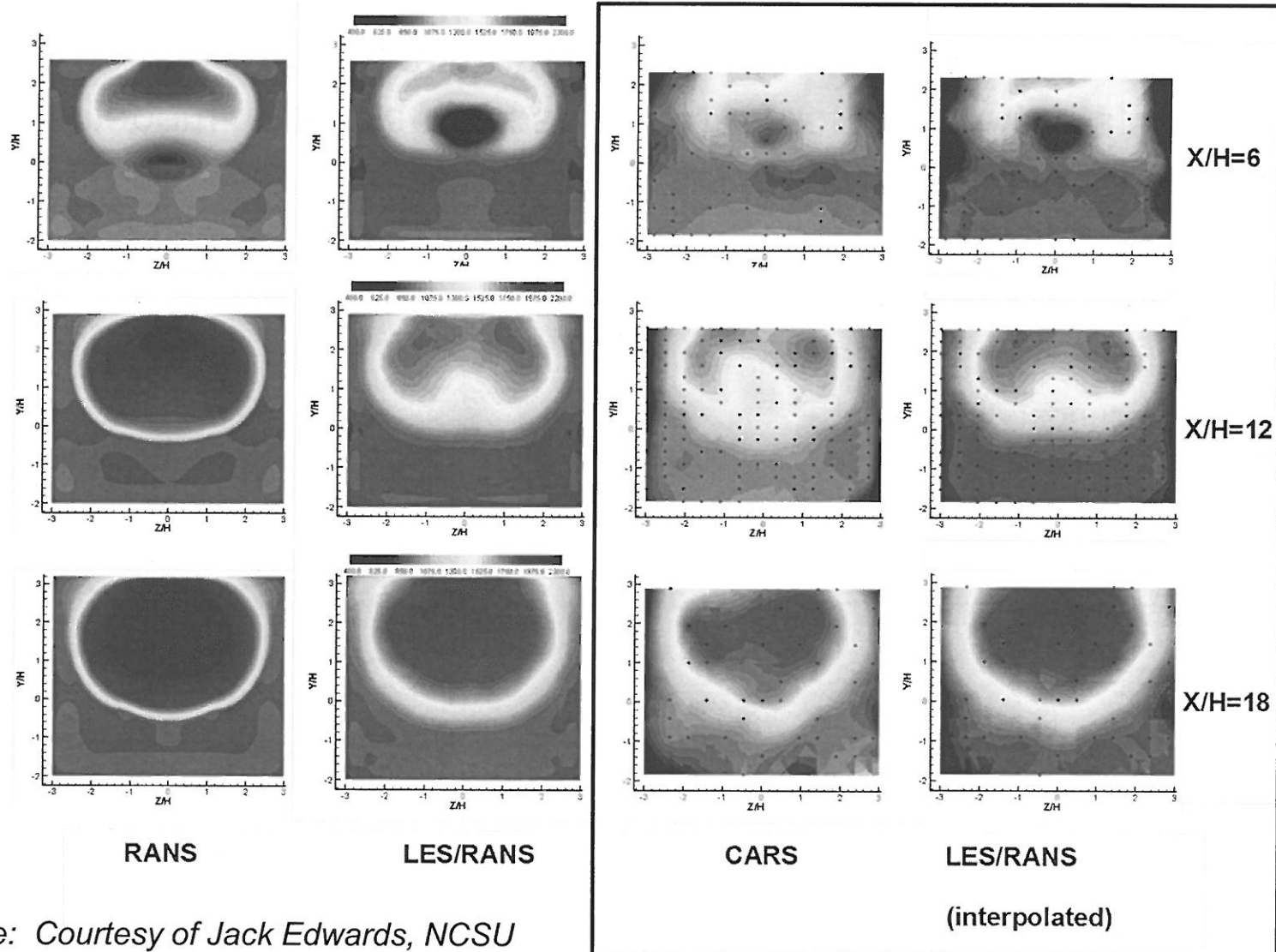


Figure: Courtesy of Jack Edwards, NCSU



Compressible Mixing



- Most recent free shear layer mixing research has been in support of jet aeroacoustics research (subsonics and supersonics).
- Practical state-of-the-art for RANS is also two-equation modeling.
- Some research in variable Pr_t for hot jet cases.
- Most research support is towards LES-based methods.
- Key LES issues:
 1. Inflow boundary treatment
 2. Grid resolution/sensitivity
 3. Farfield noise propagation techniques.



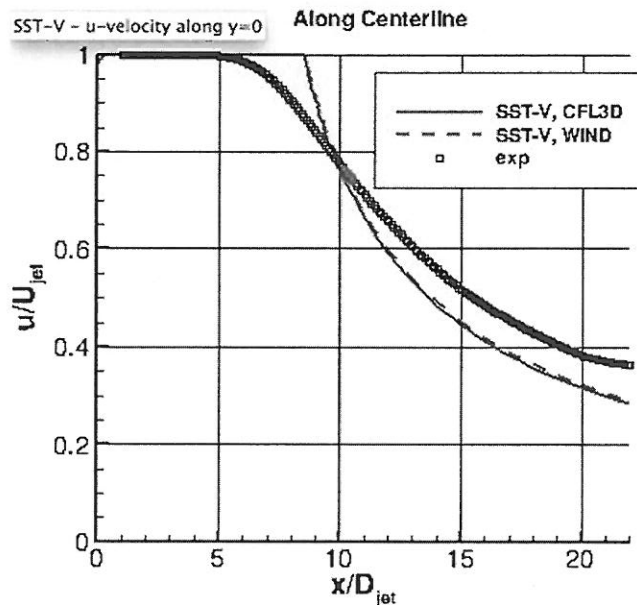
Jets and Mixing - RANS



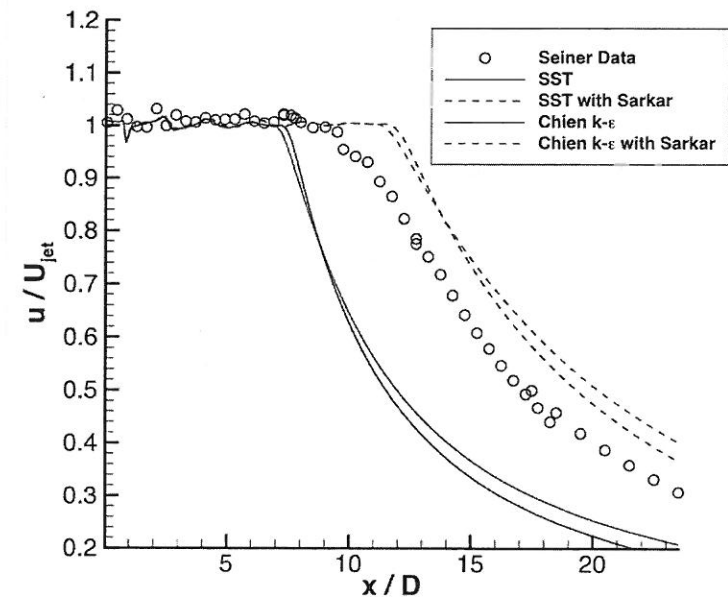
RANS Findings:

- RANS **underpredict** mixing for incompressible jets – initial shear layer is difficulty.
- Uncorrected RANS models **overpredict** mixing rate for supersonic jets and mixing layers.
- Effects of temperature and 3D jet effects are not modeled correctly.
- Compressibility corrections (i.e. Sarkar) are highly empirical and do not reproduce correct fluid dynamic effects.

Mach 0.5 Jet



Mach 2.0 Jet



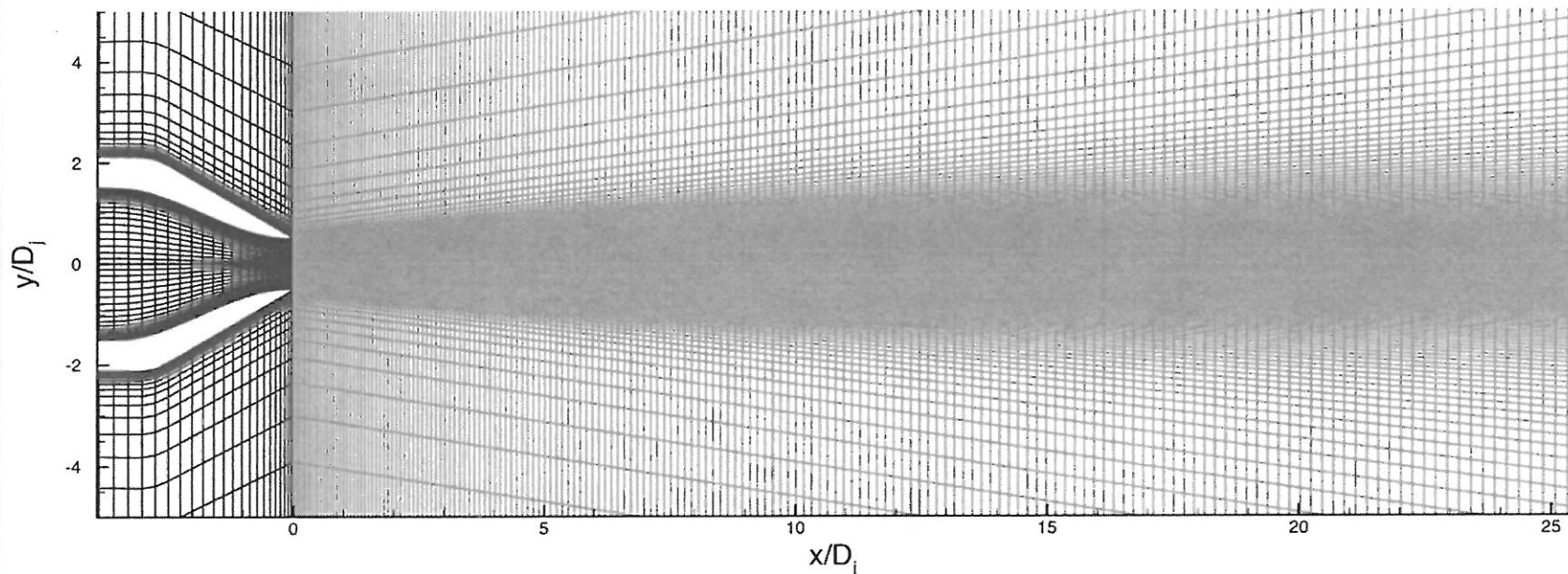


Jet Mixing - LES



- **Acoustic Reference Nozzle (ARN) and Simple Metal Chevron (SMC) configurations – tested at GRC, investigated by several LES researchers.**
- Two Mach 0.9 jet simulations considered here: (1) DeBonis (GRC) DRP with 4 stage RK, 3.5 - 9.2 million points and (2) Uzun (FSU), 4th order compact scheme with 4 stage RK, 50 - 400 million points.

DeBonis (GRC) grid:

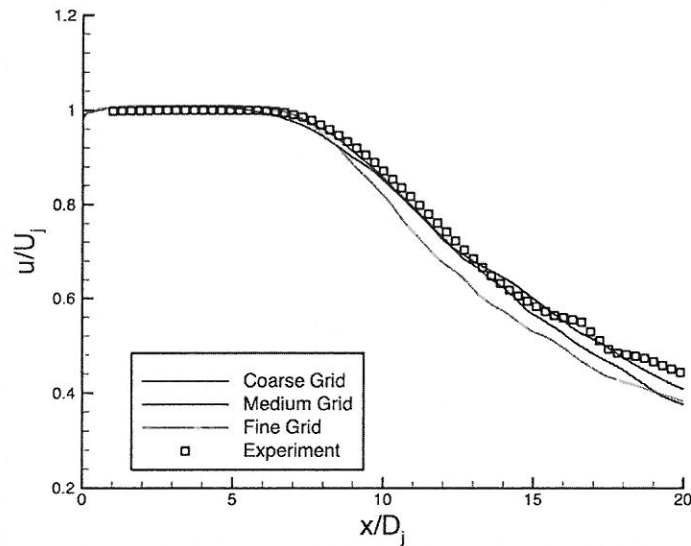




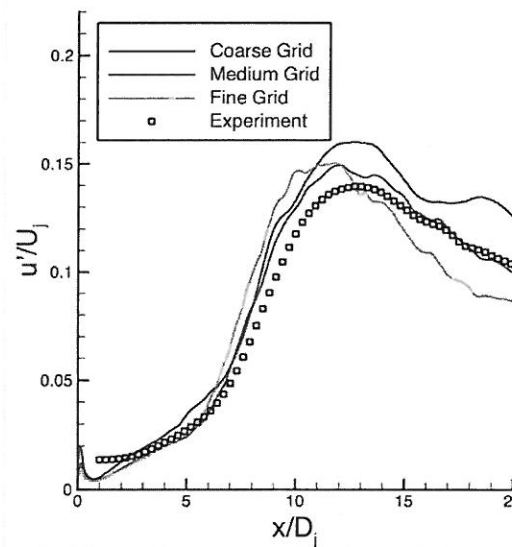
ARN - Centerline Statistics (GRC)



Mean Axial Velocity



Axial Turbulent Intensity



Radial Turbulent Intensity

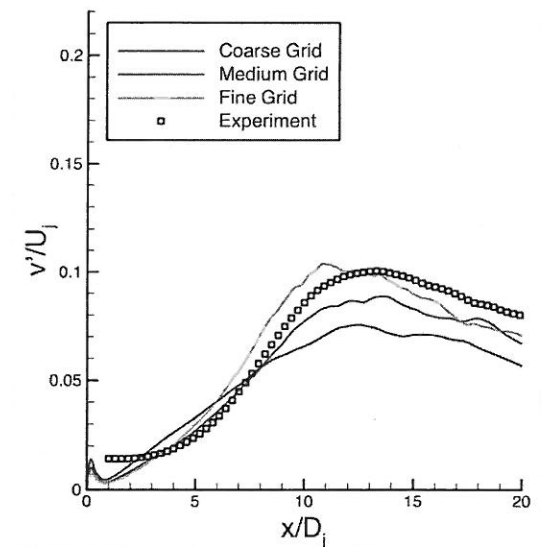


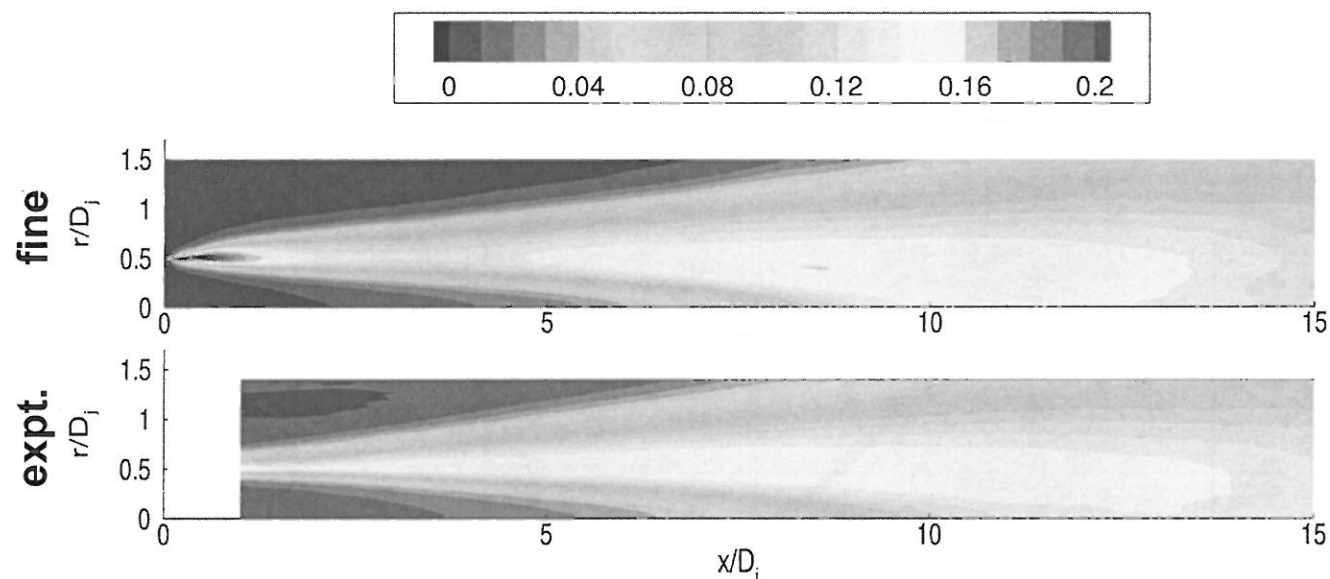
Figure: Courtesy of Jim DeBonis, NASA GRC



Turbulence Intensity Comparisons



Axial Turbulent Intensity



Radial Turbulent Intensity

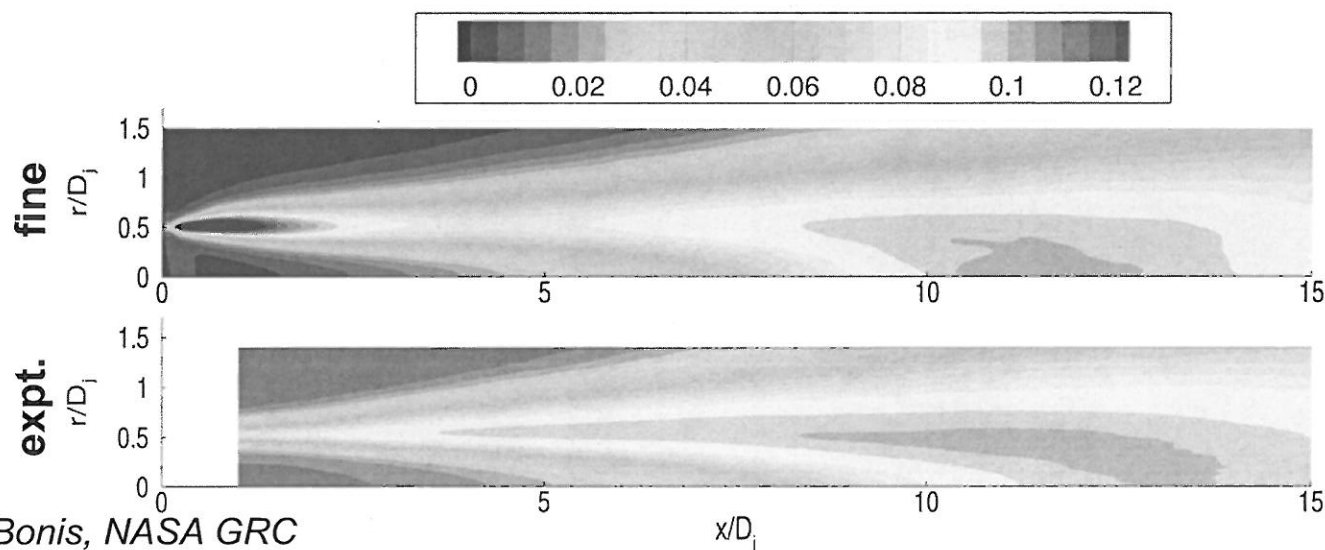


Figure: Courtesy of Jim DeBonis, NASA GRC



SMC – Jet Decay and Acoustic Radiation

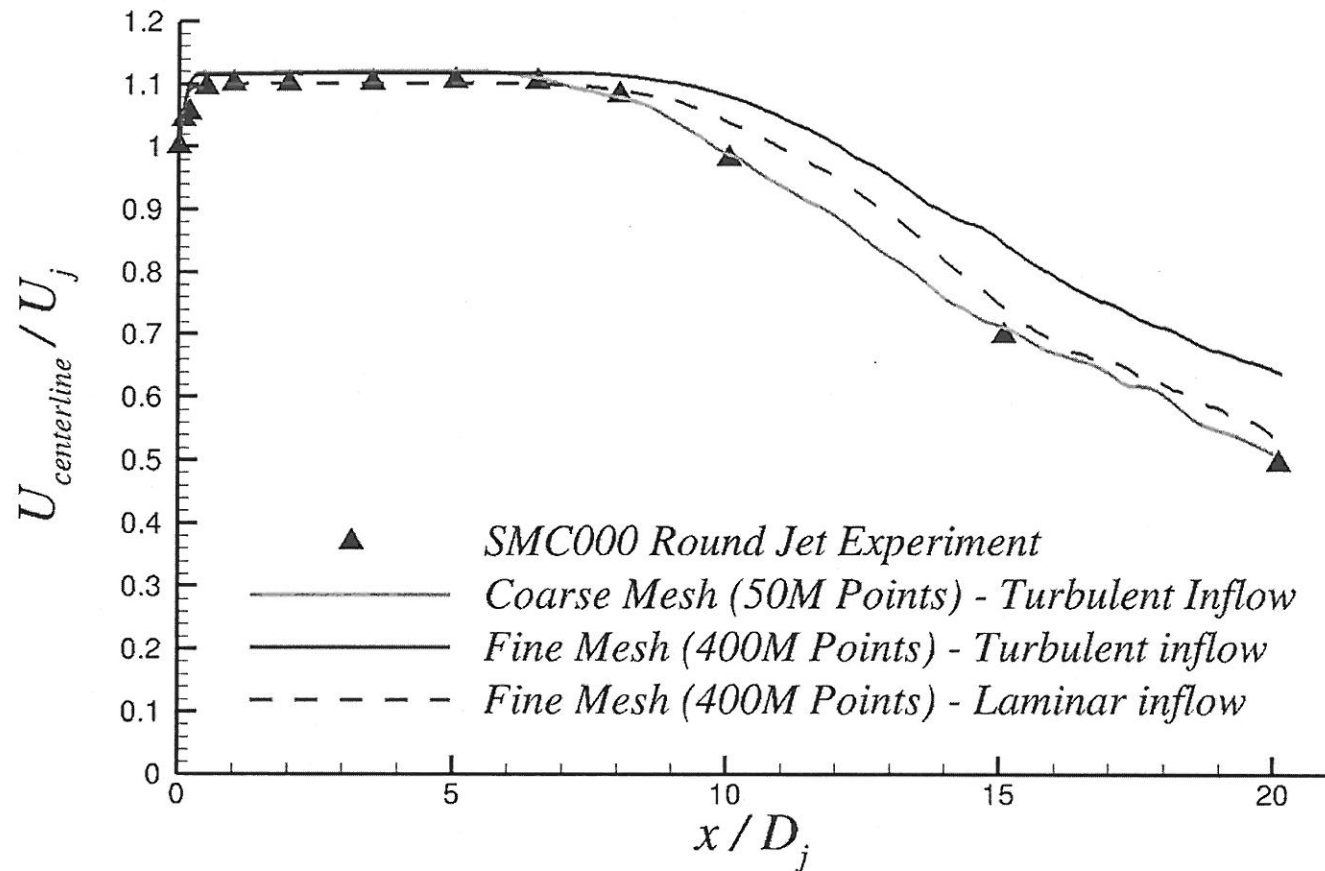


Figure: Courtesy of Ali Uzun, FSU



SMC – Jet Decay and Acoustic Radiation

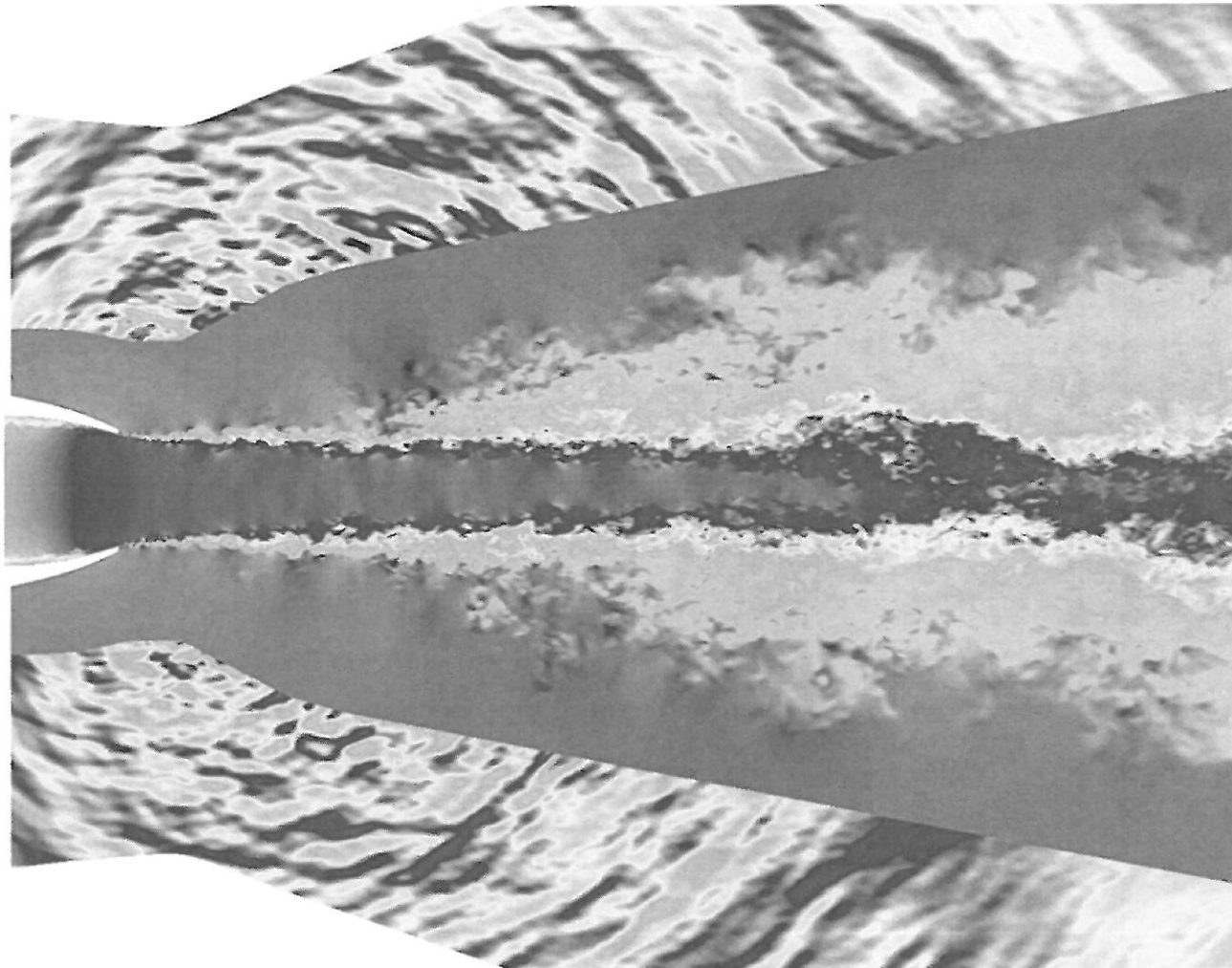


Figure: Courtesy of Ali Uzun, FSU



Combustor/Exhaust System Modeling Enhancement Needs



- **RANS:**

- Better prediction of 3D, compressible mixing; highly separated/recirculating flow in flameholder/cavity, SWTBLIs, turbulent-chemistry interactions.
- More accurate boundary conditions for thermal state.
- Variable Pr_t and Sc_t capability.

- **LES:**

- Capability to handle wall bounded and free shear layer regions. Hybrid RANS/LES methods are under investigation – but location of RANS-to-LES switch has significant effect.
- Significant uncertainty remains in how to best perform jet/mixing simulations. Highly desirable to establish “best practices” if possible.
- Models for turbulent/chemistry interactions, i.e. Filtered Density Functions (FDFs).



Experimental – Validation Data Needs



- **Centerline pressure distributions are not sufficient for validation / calibration of turbulent flow CFD. There are too many interacting features in scramjet flowpaths – unlike subsonic/transonic aerodynamics.**
- **More complete turbulent statistics for momentum, thermal, and species transport are needed.**
- **Advanced Diagnostics: CARS, PLIF, PIV – for unit problems, then more complex cases.**
- **Quantify uncertainty – e.g. PIV is powerful technique, but prone to high uncertainty in crucial regions such as initial mixing regions.**
- **Consider revisiting experiments such as Burrows-Kurkov with the advanced techniques.**
- **Design experiments to avoid contamination of focus region – i.e. SWBLI cases – nearly all experiments are in small tunnels where sidewall separations dominate region of interest.**



Conclusions



- Many extremely difficult challenges remain in turbulence modeling for air-breathing propulsion flows.
- Status of RANS Modeling for high speed propulsion flowpaths: Not much advancement in practical state-of-the-art in 2 decades.
- Dominant features of 3-D flow, large separations, SWTBLIs, chemically reacting flow, compressibility, turbulent transport of heat and species – overwhelm the capabilities of current RANS methods.
- Tweaking one turbulence modeling parameter while holding all others fixed until centerline pressure distribution matches experimental data (typical practice for scramjets) is of minimal value.
- LES and related methods are demonstrating some promise, but have their own modeling issues and (1) are not of sufficient maturity for most problems, (2) computing power is not readily available to use in a production engineering environment, (3) minimal consistency between groups in how to achieve most accurate results.